On the Constitution of Alloys of Copper, Aluminium and Silicon.

By Chiuyo Hisatsune.

Synopsis.

After a brief summary of recent work on the binary alloys of copper-aluminium, aluminium-silicon, and copper-silicon, the constitution and structure of the whole ternary system copper-aluminium-silicon are considered. The constituents present, are those of the each binary system. There exist eleven surfaces of the primary separation, and eight invariant points on the liquidus surface. Seven invariant reactions and six ternary polymorphic changes take place in the solid state. The limit of solubility of silicon and aluminium in solid copper has been also determined.

Part I. The Constitution of Binary Alloys of the Cu-Al, Al-Si and Cu-Si Systems.

I. The Equilibrium Diagram of the Copper-Aluminium System.

The first report of this ternary equilibrium diagram, the investigation of binary Cu-Al alloys, was published in the summer of 1934. The present work has been carried out through knowledge of this binary system. The complete diagram is shown in Figure 11 in that paper.*

II. The Binary Diagram of the Aluminium-Silicon System.

Alloys of the Aluminium-Silicon system are very important materials in industries. The eutectic alloy especially, makes a good light casting which is refined by the modifying treatment. Reports, therefore, of an enormous amount of investigation on the equilibrium diagram of this system have been published since Fraenkel's[13] work appeared in 1908. This author found it to be a purely eutectiferous system with no compounds and practically no solid solutions on the aluminium side. The eutectic composition was considered to lie at 10.5% silicon and at a temperature of about 578°C. Other important researches of this system, either on the solidification or on the solubility of silicon in aluminium, are those by Rosenhain, Archbutt and Hanson in 1921[14]; Edwards in 1923[15]; Otani in 1925[16]; Gwyer and Phillips in 1926[17]; Köster and Müller in 1927[18]; and Dix and Heath in 1928[19].

The present writer also had published a report[20] in 1924. Figure 12 shows the diagram

Fig. 12.

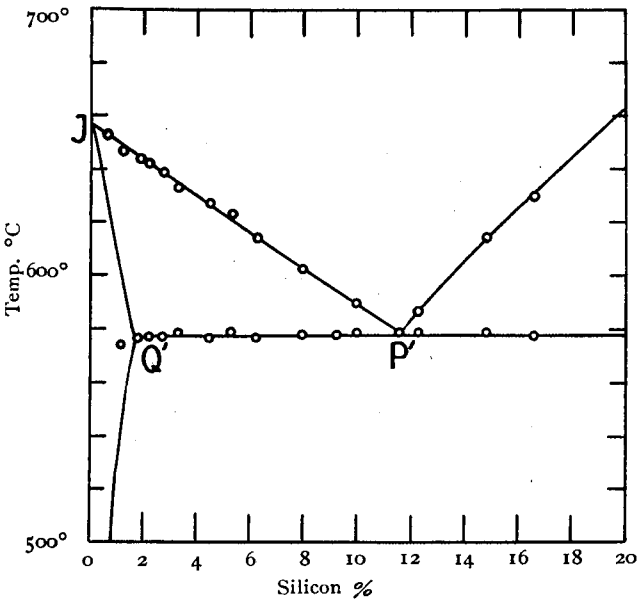

of this system ascertained by the present writer.

The liquidus of this part of the system agrees in the main with the result obtained by Edward. The eutectic point between aluminium and silicon was found to exist at 578°C, its composition being 11.62 per cent. of silicon.

III. The Binary Diagram of the Copper-Silicon System.

Concerning this binary system, Rudolfi[21] published in the first place an investigation of the equilibrium diagram in 1907. Afterward Sanfourche,[22] Corson,[23] and Matsuyama[24] also studied the binary system, and recently Smith[25] published a

* Memoirs of the College of Engineering, Kyoto Imp. Univ., Vol. VIII, No. 2, P. 74.

13) Z. anorg. Chem., **58** (1908) 154.
14) Eleventh Report of Alloy Research Committee of Mechanical Engineers (1921)
15) Chem. & Met. Eng., **28** (1923) 165.
16) Kinzoku no Kenkyu **2** (1925) 212.
17) J. Inst. Metals, **36** (1926) 283.
18) *Z.* Metallkunde, **19** (1927) 52.
19) Am. Inst. Min. Met. Eng. Metal Division, (1928) 164.
20) Suiyo Kwaishi **4** (1924) 456.
21) Z. anorg. Chem., **53** (107) 216.
22) Rev. Met. **16** (1919) 246.
23) Proc. Inst. Metals Div. (1927) 435.
24) Kinzoku no Kenkyu **3** (1926) 86.
25) Amer. Inst. Min. Met. Eng., (1927) 414.

very complete and accurate diagram which is reproduced in Figure 13.

Fig. 13.

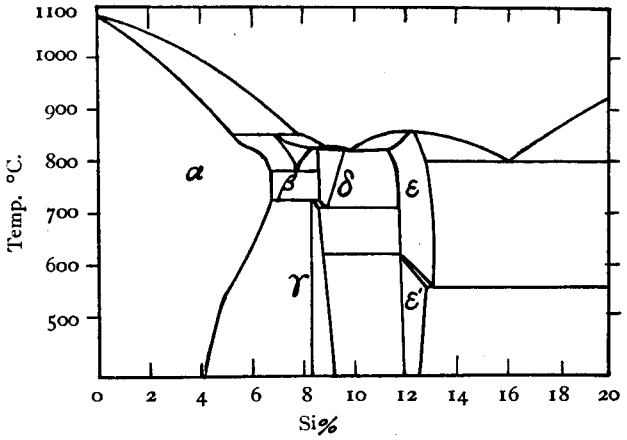

According to Smith the following phenomena were ascertained :—

(1) the phase β is formed by the reaction of α with 5.25 per cent. and liquid with 7.7 per cent. of silicon and it always decomposes eutectoidally into $\alpha+\delta$ at 782°C.; (2) at 824°C. the saturated β (approximately 8.4 per cent. of silicon) reacts with liquid and produces the δ phase with 8.6 per cent. of silicon. This phase decomposes to $\gamma+\varepsilon$ at 710°C.; (3) the phase γ is formed at 726°C. by a peritectoid reaction between δ and α; (4) a eutectic point between the δ phase and the next phase ε exists at 820°C. and 9.9 per cent. of silicon. The ε phase crystallizes directly from the melts at 859°C. and 12.3 per cent. of silicon. It has a polymorphic transformation, $\varepsilon \rightleftarrows \varepsilon'$, and (5) a eutectic point between the ε phase and silicon was found to exist at 802°C., its composition being 16.0 per cent. of silicon.

In 1931 Iokibe[26] corrected Smith's diagram by means of thermal analysis, the measurement of electric resistance and microscopic examination as shown in Figure 14.

Fig. 14.

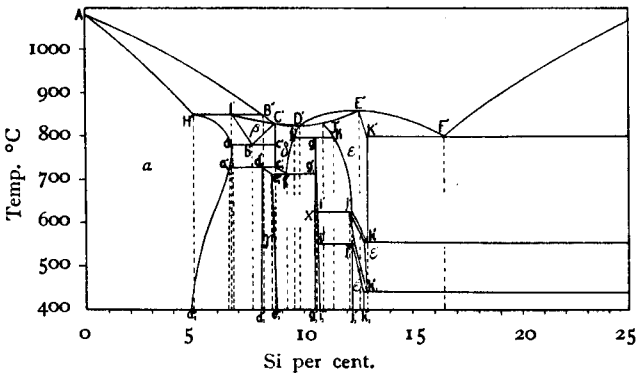

The results of Iokibe's experiments are almost in accordance with Smith, but Iokibe discovered a new phase which was called the X phase. The phase X is formed at 800°C. by a peritectoid reaction between the δ and ε phases. This author also found that the phase ε has two polymorphic changes, $\varepsilon \rightleftarrows \varepsilon'$ and $\varepsilon' \rightleftarrows \varepsilon''$.

As the experiments of Iokibe are considered to be sufficiently accurate, the present writer did not think it necessary to investigate the diagram further.

Part II. The Constitution of the Alloys of Copper, Aluminium and Silicon.

I. Introduction.

The constitution of this whole system has not been thoroughly investigated, but the equilibrium diagram of the aluminium-rich corner has been ascertained by some investigators.

Goto and Mishima[27] determined the constitution of these alloys containing copper up to 40 per cent. and silicon up to 16 per cent. In this range there is a ternary eutectic point at 517°C between aluminium, silicon and $CuAl_2$.

Fuss[28] stated that a ternary eutectic point between aluminium, silicon and $CuAl_2$ exists at 520°C., its composition being 65.8 per cent. of aluminium, 29 per cent. of copper, and 5.2 per cent. of silicon.

In the year 1928 the present writer[29] reported an investigation of this system which covered the range 0–70 per cent. of copper and 0–8 per cent. of silicon. Thermal curves were taken of a series of alloys containing 2, 4, 6 and 8 per cent. of silicon, in which the copper content varied in steps of 5 per cent., or less, according to the complexity of the sectional diagrams. Two peritecto-eutectic reactions, Liquid $+\eta \rightleftarrows$ CuAl + Si, Liquid + CuAl $\rightleftarrows$ $CuAl_2$ + Si, were found to occur at 611° and 573°C. respectively, and a ternary eutectic point between aluminium, $CuAl_2$ and silicon was determined to exist at 522°C, its composition being 23.8 per cent. of copper, 5 per cent. of silicon and 71.2 per cent. of aluminium.

Gwyer, Phillips and Mann[30] studied in the same year the alloys containing 0–50 per cent. of copper and 0–20 per cent. of silicon. They stated that there exists a ternary eutectic point between aluminium, $CuAl_2$ and silicon at 525°C., its composition being 26 per cent. of copper, 6.5 per cent. of silicon and 67.5 per cent. of aluminium.

26) Kinzoku no Kenkyu **8** (1931) 433.
27) J. Min. Met. Japan, **41** (1925) 4.
28) Z. Metallk. **16** (1924) 362.
29) Suiyo Kwaishi, **5** (1928).
30) J. Inst. Metals, **40** (1928) 297.

Recently Urazov, Pogodin and Zamoruew[31] determined the constitution of the ternary alloys in concentrations up to 24 per cent. of silicon and 40 per cent. of copper. The ternary eutectic has the following composition and temperature; Si 5%, Cu 27% and Al 68%, and 525°C. The boundary of the ternary solid solutions of copper and silicon in aluminium at different temperature was also determined by microscopic examination of the quenched alloys.

With the exception of the present writer's previous investigation, no work on the constitution of aluminium rich Al-Cu-Si alloys has been carried out in such wide range.

The constitution of the ternary copper-rich Cu-Al-Si system has not been studied hitherto, but some properties of silicon-" Aluminium-Bronze " have been investigated. Shiozawa[32] has examined the mechanical properties and microstructure of a number of copper alloys containing 2 to 10 per cent. of aluminium and a small proportion of silicon. Sevault[33] has studied the influence of 0.43 to 4.31 per cent. of silicon on the transformation points, physical properties and microstructure of copper alloys containing 8.6 to 13 per cent aluminium.

More recently, Brice[34] has also examined the Brinell hardness, mechanical properties and microstructure of three typical copper-aluminium alloys, containing respectively 5.0, 7.25, and 10.0 per cent. of aluminium, with the addition to each of up to 5.0 per cent. of silicon. The alloys have been examined in the chill-cast condition, and also after subjection to mechanical and heat-treatment.

In short the whole constitution of the ternary system of copper, aluminium and silicon seems not to have been investigated and therefore an attempt was made, as described below, to ascertain it.

II. Materials Employed, Preparation of Specimens and Experimental Method.

The alloys for the present investigation were made from electrolytic copper, alumininm 99.8 per cent. pure and the purest silicon obtainable in our country. The latter, which was refined by boiling with aquea regia, had the following analysis; Si 98.74%, Fe 0.83%, Al 0.22%.

The silicon was usually added in the form of intermediate alloys. Two kinds of such hardener were prepared as follows: copper alloys with 10 and 24 per cent. of silicon were used for the copper corner alloys and aluminium alloys with 10, 15 and 25 per cent. of silicon for the aluminium corner alloys.

Thermal analysis employed were identical with those described in the previous investigation of the alloys of copper with aluminium.

III. The Constitution of the Copper-rich Cu-Al-Si System.

A. Thermal Analysis.

(1) Phenomena of Solidification.

Thermal curves were taken for two groups of alloys, the first comprising a series of alloys containing 1, 2, 4, 6, 10, 12 and 20 per cent. of silicon in which the copper content varied in steps of 1 per cent., or more, according to the constitutional sections; and the second comprising the alloy series whose aluminium content was constant and whose silicon content varied in steps of 1 per cent., from 7 to 15 per cent. The aluminium content of the second group varied in steps of 1 per cent. from zero to 8.

Table 9.

TSA 1 Series. (1% Silicon).

No.		Composition. (by analysis)			Points of Change or Arrest. °C.				
		Cu%	Si%	Al%					
TSA	107	91.96	1.07	Rest	1028				
,,	109	89.46	1.25	,,	1019	518			
,,	110	88.77	1.16	,,	1020	508			
,,	111	87.80	1.19	,,	1027	572	512		
,,	112	86.54	1.15	,,	1032	510			
,,	113	85.85	1.03	,,	1028	518			
,,	114	84.80	1.09	,,	1026	950	880		
,,	115	83.63	1.25	,,	1021	980			
,,	116	82.43	1.01	,,	1016	930			
,,	117	81.85	1.17	,,	1002	926	845		
,,	118	80.38	1.02	,,	996	844	820	770	
,,	119	79.59	1.26	,,	990	920	850	770	
,,	120	78.82	0 99	,,	968	916	846	746	
,,	121	78.10	1.02	,,	946	910	830	746	680
,,	122	76.78	1.14	,,	930	920	838	742	722
,,	123	75.86	1.27	,,	916	840	735		
,,	124	75.12	1.30	,,	894	844	714	572	
,,	125	73.88	1.19	,,	876	697	580		
,,	126	73.11	1.04	,,	868	690	600	580	
,,	127	71.86	1.24	,,	838	650	610	590	570
,,	128	70.73	1.26	,,	824	638	606	596	568
,,	130	68.89	1.28	,,	788	606	603	570	558
,,	132	66.87	1.28	,,	751	610	608	571	558
,,	133	65.51	1.33	,,	733	610	571	556	
,,	135	63.95	1.08	,,	710	615	580	556	

31) Mineralnoe Suiré *i* Tzvetnuie Met. **4** (1929) 160, C. A. 25 (1931) 1785.
32) J. Min. Met. Japan, **45** (1929) 217.
33) Rev. Mét., **27** (1930) 154.
34) J. Inst. Metals, (1931).

The temperatures of the arrests found on cooling curves are given in Tables 9 to 21, and plotted in Figures 15 to 26, where they are represented by the symbol o.

Table 10.

TSA 2 Series. (2% Silicon).

No.	Composition. (by analysis)			Points of Change or Arrest. °C.				
	Cu%	Si%	Al%					
TSA 206	92.11	2.05	Rest	1016				
„ 208*	90	2	„	1008				
„ 210	87.71	2.01	„	1016	520			
„ 211	86.82	2.17	„	1020	518			
„ 212	85.88	1 92	„	1009	910	520		
„ 213	84 92	2 24	„	1008	946			
„ 214	83.91	2.05	„	999	980			
„ 215	82.91	1.69	„	990	780			
„ 216	82.00	2.03	„	988	770			
„ 217	81.28	2.03	„	988	816	760		
„ 218	80.17	1.85	„	975	832	762		
„ 219	79.39	1.80	„	955	923	843	762	
„ 220	78.39	1.73	„	935	843	758		
„ 221	76.95	2.09	„	923	840	756	748	688
„ 222	76.05	2 00	„	907	846	752	679	
„ 223	75.00	2.03	„	885	744	570		
„ 224	73.77	2.20	„	875	730	680	582	
„ 225	73.00	1.98	„	835	727	670	590	
„ 226	71.95	2.14	„	818	730	650	600	590
„ 227*	71	2	„	810	690	606	570	
„ 228	70.25	2.11	„	785	675	602	562	
„ 229	68.80	2.15	„	772	640	595	557	
„ 230*	68	2	„	764	630	606	594	575
„ 231	66 82	2.21	„	738	609	600	568	
„ 232	66.02	1.87	„	718	618	605		570

* Not analyzed. Composition given as charged.

Table 11.

TSA 4 Series. (4% Silicon).

No.	Composition. (by analysis)			Points of Change or Arrest. °C.					
	Cu%	Si%	Al%						
TSA 405	91.10	4.12	Rest	994	960	700			
„ 406	89.97	4.03	„	984	756	666			
„ 407	88.66	4.26	„	985	686	652			
„ 408	88.06	4.23	„	987	595	572			
„ 409	87.05	4 25	„	993	555				
„ 410	86.17	4.26	„	991	540				
„ 411	84.97	4.18	„	987	522				
„ 4·2	84.28	4.00	„	978	937				
„ 413	82.98	4.01	„	977	790				
„ 414	82.11	3.89	„	975	772				
„ 415	80.96	3.90	„	967	780				
„ 416	79.65	4.23	„	963	780				
„ 417	79.05	4.31	„	950	770				
„ 418*	78	4	„	930	763				
„ 419	77.14	4.28	„	920	762				
„ 420	75.73	4.28	„	900	758				
„ 421	74.92	3 87	„	886	853	758	753		
„ 422*	74	4	„	872	753				
„ 423	72.91	4.00	„	864	750				
„ 424	71.95	3.92	„	838	740				
„ 425	70.96	4.15	„	830	736	650	574	564	
„ 426*	70	4	„	818	728	610	600	574	
„ 428	68.13	4 03	„	780	695	608	565		
„ 430	66.09	4.21	„	740	672	608	598	570	558

* Not analyzed. Composition given as charged.

Table 12.

TSA 6 Series. (6% Silicon).

No.	Composition. (by analysis)			Points of Change or Arrest. °C.				
	Cu%	Si%	Al%					
CS 7	Rest	6.42	—	919	850	784		
TSA 601	93.15	5.59	Rest	927	871	810	766	
„ 602	92.28	5.79	„	914	897	781		
„ 603	91.33	5.49	„	914	759	747		
„ 604	90.16	5.62	„	907	678	656	480	
„ 605	89.18	5.76	„	917	684	656	490	
„ 606	88.30	5.63	„	915	641	480		
„ 607	87.13	5.80	„	912	858			
„ 608	86.42	5.58	„	910	874			
„ 609	85.41	5.67	„	905	896	750	568	506
„ 610	84.32	5.71	„	897	742	538		
„ 611	83.35	5.56	„	896	751	510		
„ 612	82.41	5.48	„	890	760			
„ 613	81.50	5.53	„	884	767			
„ 615*	79.00	6.00	„	862	772			
„ 618*	76.00	6.00	„	846	760			
„ 620	74.08	5.88	„	835	750	669		
„ 623	70.68	5.90	„	800	732	662	600	550
„ 625*	69.00	6.00	„	775	730	610	590	
„ 629*	65 00	6.00	„	716	706	599	588	562
„ 630*	64 00	6.00	„	697	658	600	575	563

* Not analyzed. Composition given as charged.

Table 13.

TSA 10 Series. (10% Silicon).

No.	Composition. (by analysis)			Points of Change or Arrest. °C.				
	Cu%	Si%	Al%					
CS 10	Rest	9.97	—	825	820	710		
TSA 1001	89.10	10.05	Rest	822	620			
„ 1002	87.93	9.89	„	816	814	676		
„ 1003	87.04	10.11	„	817	806	666		
„ 1004	85.95	9.87	„	822	804	630		
„ 1005	85.00	10.21	„	830	790	740	570	
„ 1006	83.88	10.00	„	814	758	725	577	
„ 1008	82.15	10.23	„	790	734	725	580	530
„ 1009*	81	10	„	778	740			
„ 1010	80.03	10.31	„	756				
„ 1011	79.30	10.05	„	762	750			

„	1012	78.08	10 18	„	770	758			
„	1013*	77	10	„	778	762			
„	1014	76	10	„	780	768			
„	1015	75.21	10 26	„	788	780			
„	1020*	70	10	„	812	763			
„	1025*	65	10	„	805	740	605	560	
„	1030*	60	10	„	796	701	607	572	

* Not analyzed. Composition given as mixed.

Table 14.

TSA 12 Series. (12% Silicon).

No.	Composition. (by analysis)			Points of Change or Arrest. °C.				
	Cu%	Si%	Al%					
CS 12	Rest	11.33	—	847	820	700		
TSA 12005	88.08	11.41	Rest	847	652			
„ 1201	87.13	11.81	„	837	814	659		
„ 1202	86.58	11.37	„	820	807	638		
„ 1203*	85	12	„	798	786	727	626	571
„ 1204*	84	12	„	767	727	620	568	
„ 1205	83.69	11.43	„	735	727	578	536	
„ 1206	82.63	11.30	„	729	727	578	536	
„ 1208*	80	12	„	770	744	578	528	
„ 1210*	78	12	„	777	756	570	528	
„ 1212*	76	12	„	806	767			
„ 1215*	73	12	„	824	774			
„ 1220*	68	12	„	836	760			
„ 1225*	63	12	„	824	731	561		
„ 1230*	58	12	„	806	681	608	572	553
„ 1235*	53	12	„	792	648	608	578	
„ 1240*	48	12	„	767	583	572		

* Not analyzed. Composition given as mixed.

Table 15.

TSA 20 Series. (20% Silicon).

No.	Composition. (by charge)			Points of Change or Arrest. °C.			
	Cu%	Si%	Al%				
CS 20	80	20	—	908	800		
TSA 2005	75	20	Rest	926	760	730	
„ 2010	70	20	„	984	760	750	
„ 2015	65	20	„	970	770		
„ 2020	60	20	„	968	760	742	565
„ 2025	55	20	„	955	760	742	570
„ 2030	50	20	„	935	710	608	570
„ 2040	40	20	„	875	570	525	
„ 2050	30	20	„	827	549	522	
„ 2060	20	20	„	778	525		
„ 2070	10	20	„	730	556	522	
„ 2075	5	20	„	755	564	522	
AS 20	—	20	80	678	579		

Table 16.

T 1 Series. (1% Aluminium).

No.	Composition. (by analysis)			Points of Change or Arrest. °C.				
	Al%	Si%	Cu%					
T 14	Rest	3.88	94.95	995	850			
„ 15	„	4.72	94.24	966	859	817		
TSA 601	„	5.59	93.15	927	871	810	766	
T 16.5	„	6.10	92.77	914	865	817	769	
„ 17	„	6.63	92.34	883	874	787	767	650
„ 17.5	„	7.21	91.55	862	768	760	651	
„ 18	„	7.98	90.77	845	757	650		
„ 18.5	„	8.33	90 51	831	824	650		
„ 19	„	8.78	90.11	825	618			
„ 19 5	„	9.07	89.77	824	638			
„ 110	„	9.72	89.26	824	820	816	688	619
„ 110.5*	„	10.5	88.5	821	816	749	691	615
„ 111	„	10.84	88.12	826	817	691	581	
„ 111.5	„	11.36	87.54	835	817	687		
TSA 1201	„	11.81	87.13	837	814	659		
T 112.5*	„	12.5	86.5	836	570			
„ 113.5	„	13.19	85.76	826	760	637	582	
„ 115*	„	15	84	808	781			
„ 117*	„	17	82	806	787			

* Not analyzed. Composition give as mixed.

Table 17.

T 2 Series. (2% Aluminium).

No.	Composition. (by analysis)			Points of Change or Arrest. °C.			
	Al%	Si%	Cu%				
TSA 602	Rest	5.79	92.28	914	897	781	
T 27	„	6.87	90.95	885	749	576	
„ 27.5	„	7.25	90.67	883	856	746	576
„ 28	„	8.03	89.86	856	732	588	
„ 28.5	„	8 42	89.39	839	824	577	
„ 29	„	8.71	89.11	826	818	549	
„ 29.5	„	9.11	88.78	824	816	670	
TSA 1002	„	9.89	87.93	816	814	676	
T 210.5*	„	10.5	87.5	818	814	676	
„ 211*	„	11	87	819	810	650	
TSA 1202	„	11.37	86.58	820	807	638	
T 212*	„	12	86	820	570		
„ 213	„	12.75	85.09	815	732		
„ 215*	„	15	83	782	767	727	
„ 216*	„	16	82	781	727		
„ 217*	„	17	81	784	727		

* Not analyzed. Composition given as mixed.

Table 18.

T 3 Series. (3% Aluminium).

No.	Composition. (by analysis)			Points of Change or Arrest. °C.				
	Al%	Si%	Cu%					
TSA 603	Rest	5.49	91.33	914	759	747		
T 37	„	6.52	90.43	889	866	781	726	490

,,	38	,,	7.47	89.62	860	829	720		490
,,	39	,,	8.63	88.12	842	746			
,,	310	,,	9.71	87.07	820	808	664	641	
,,	311	,,	10.67	86.30	805	631	590		
,,	312	,,	11.28	85.84	798	726	626	571	
,,	313	,,	12.73	84.9	799	740	727		
,,	313.5*	,,	13.5	83.5	795	741	728		
,,	314*	,,	14	83	785	763	739	727	
,,	315*	,,	15	82	787	758	736	727	
,,	315.5*	,,	15.5	81.5	799	766	757	727	

* Not analyzed. Composition given as mixed.

Table 19.

T 4 Series. (4% Aluminium).

No.	Composition. (by analysis)			Points of Change or Arrest. °C.			
	Al%	Si%	Cu%				
T 45	Rest	4.63	91.50	950	710		
TSA 604	,,	5.62	90.16	907	678	656	480
T 47	,,	6.54	89.35	882	684		
,, 48	,,	7.63	88.30	860	844		
,, 49	,,	8.50	87.19	844	808		
,, 410	,,	9.65	86.16	826	816	796	633
,, 411	,,	10.86	85.26	786	727	548	
TSA 1204*	,,	12	84	767	727	620	568
T 414	,,	13.48	82.60	733	727		

* Not analyzed. Composition given as mixed.

Table 20.

T 6 Series. (6% Aluminium).

No.	Composition. (by analysis)			Points of Change or Arrest. °C.				
	Si%	Cu%	Al%					
TSA 206	2.05	92.11	Rest	1016				
TAS 604	3.88	90.04	,,	991	756	660		
T 605	4.67	89.17	,,	960	650			
,, 606	6.01	87.95	,,	912	641	480		
,, 607	6.58	87.55	,,	904	848	546	524	456
,, 608*	8.00	86.00	,,	856	611	524		
,, 609*	9.00	85.00	,,	842	754	726	578	
TSA 1006	10.00	83 88	,,	814	758	725	577	
T 611	10.62	83.16	,,	783	728	579	528	
TSA 1206	11.30	82.63	,,	729	727	578	536	
T 614*	14.00	80.00	,,	762	731			

* Not analyzed. Composition given as mixed.

Table 21.

No.	Composition. (by analysis)			Points of Change or Arrest. °C.				
	Si%	Cu%	Al%					
TSA 312	3.26	84.63	Rest	985	975			
,, 313	3.17	83.83	,,	983	980			
,, 314	3.04	82.91	,,	978				
,, 705*	7.00	88.00	,,	896	840			
,, 707*	7.00	86 00	,,	875	696	600	546	526
,, 708*	7.00	85.00	,,	869	731	586		527
,, 709*	7.00	84.00	,,	885	733	581		526
,, 710*	7.00	83.00	,,	884	741	529		
,, 711*	7.00	82.00	,,	867	755	748		516
,, 807*	8.00	85.00	,,	859	727	587		526
,, 808*	8.00	84.00	,,	856	734	580		527
,, 809*	8.00	83.00	,,	859	738	569		534
,, 810*	8.00	82.00	,,	848	748	744		
,, 907*	9.00	84.00	,,	840	727	577		546

* Not analyzed. Composition given as mixed.

From these results we observed no ternary intermetallic compound to exist but 15 definite constituents which have been determined in the investigation of each binary system were found to occur in the ternary system. They are termed α, β, γ_1, γ_a, γ_s, δ, X, ε_{1a}, ε_{2a}, ε_s, ζ_1, ζ_2, η_1, η_2 and silicon

Fig. 15. TSA 1 Series. (1% Silicon).

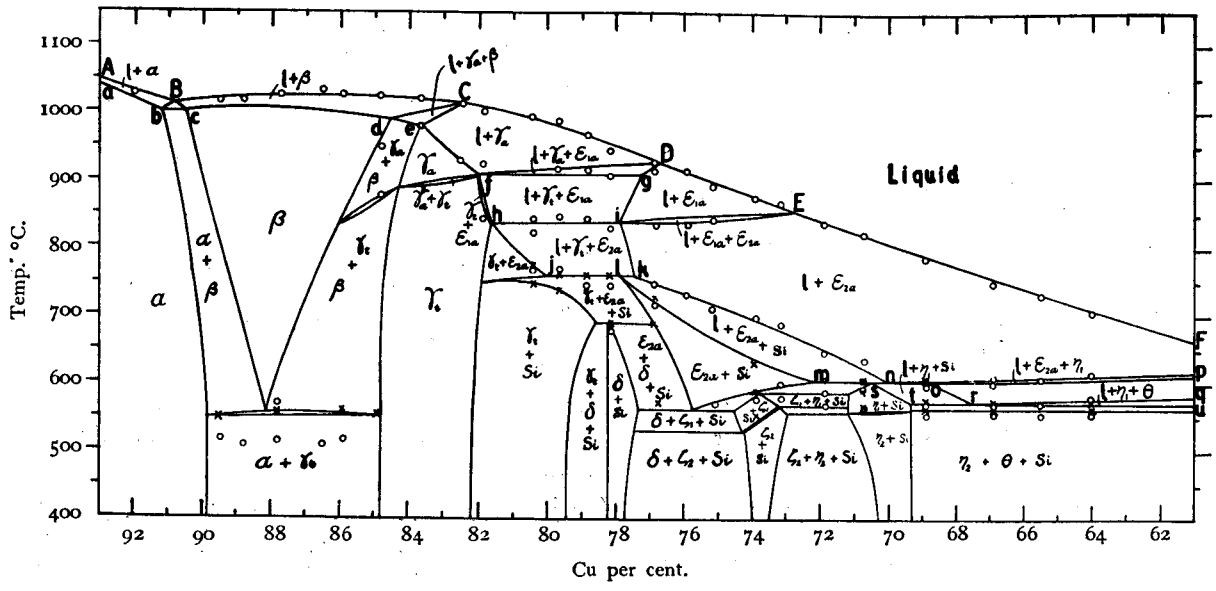

Fig. 16. TSA 2 Series. (2% Silicon).

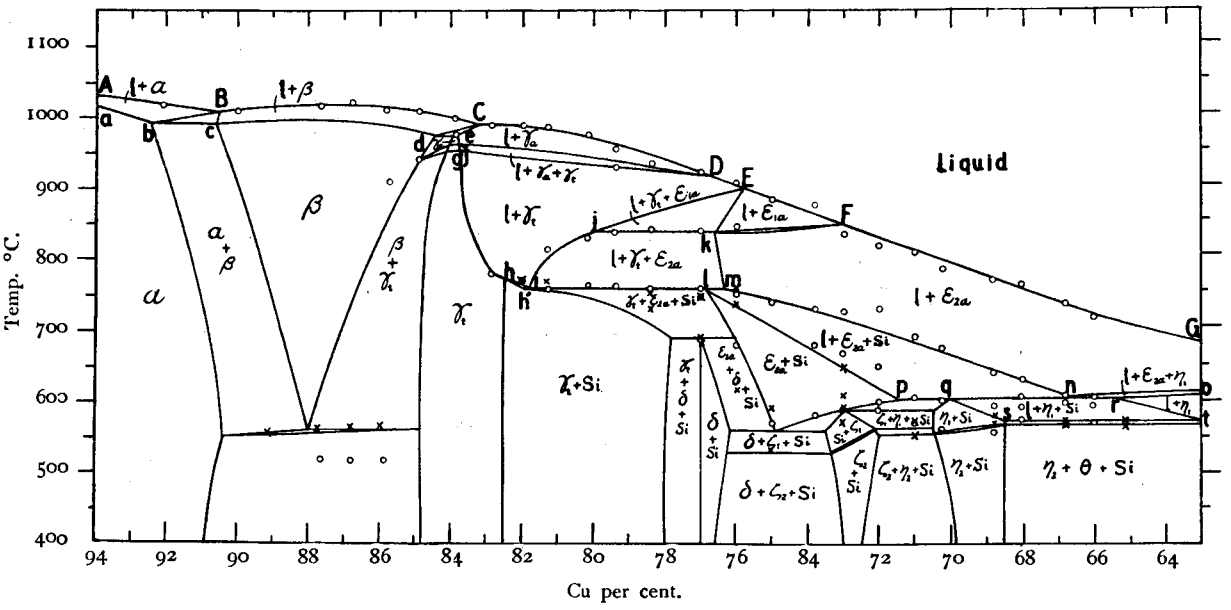

Fig. 17. TSA 4 Series. (4% Silicon).

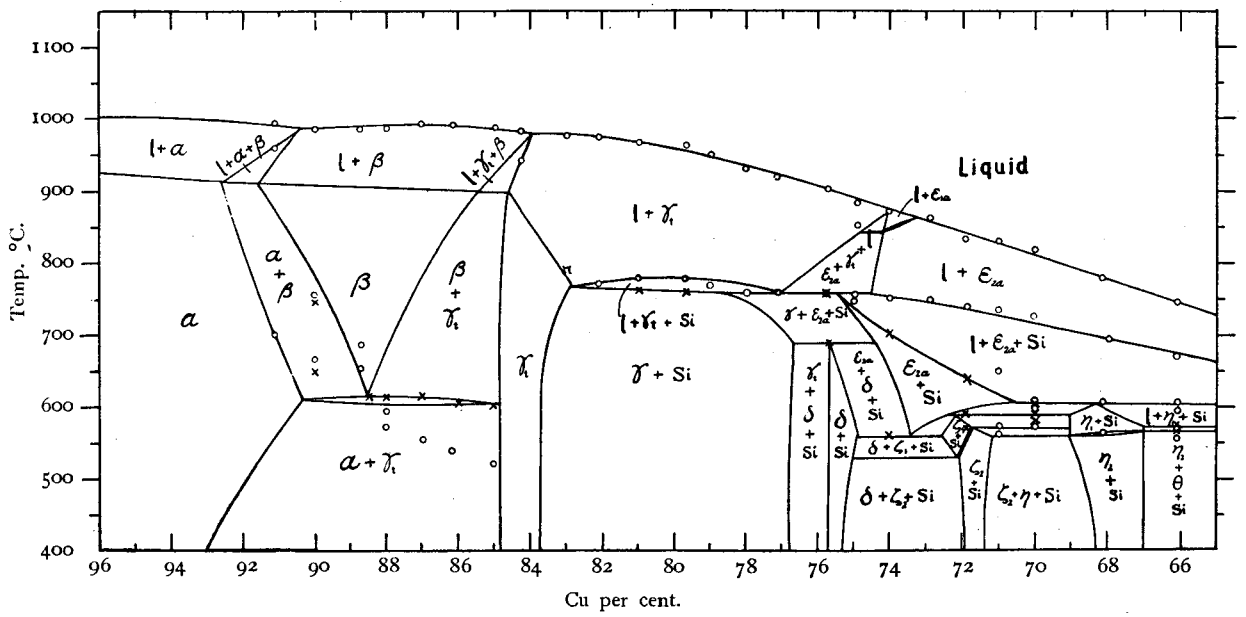

as similarly called in both copper-aluminium and copper-silicon diagrams. Among them the γ_2 phase of the copper-aluminium system (Figure 11) and the δ phase of the copper-silicon system (Figure 14) are completely soluble in all proportions: hence it is denoted as γ_t phase throughout this paper, and the phases γ_1, ε_1, ε_2, ζ_1, ζ_2, η_1 and η_2 of the Cu-Al system are termed as γ_a, ε_{1a}, ε_{2a}, ζ_1, ζ_2, η_1 and η_2 respectively. The phases γ, X and ε of the Cu-Si system are called also as γ_a, X and ε_s.

Some important sectional diagrams will be here explained. In Figure 15, the liquidus consists of several branches, of which AB represents the separation of α, BC that of β, CD that of γ_a, DE that of ε_{1a} and EF that of ε_{2a}.

The curves of the secondary crystallization consist also of several branches, of which bB represents the separation of a binary eutectic $\alpha+\beta$, cB that of $\beta+\alpha$, dC and eC the reaction of the binary complex $\beta+\gamma_a$, fD and gD that of the binary complex $\gamma_a+\varepsilon_{1a}$, gi the separation of the binary complex $\varepsilon_{1a}+\gamma_t$, iE the reaction of the binary complex $\varepsilon_{1a}+\varepsilon_{2a}$, ik that of the binary complex $\varepsilon_{2a}+\gamma_t$, kn the crystallization of the binary eutectic $\varepsilon_{2a}+$Si, np that of the binary complex $\varepsilon_{2a}+\eta_1$, op that of $\eta_1+\varepsilon_{2a}$, or that of the binary eutectic η_1+Si, and rq that of binary complex $\eta_1+\theta$. The curves of ab, bc, cd, de, ef, fh, hj, lm and st represent the

Fig. 18. TSA 6 Series. (6% Silicon).

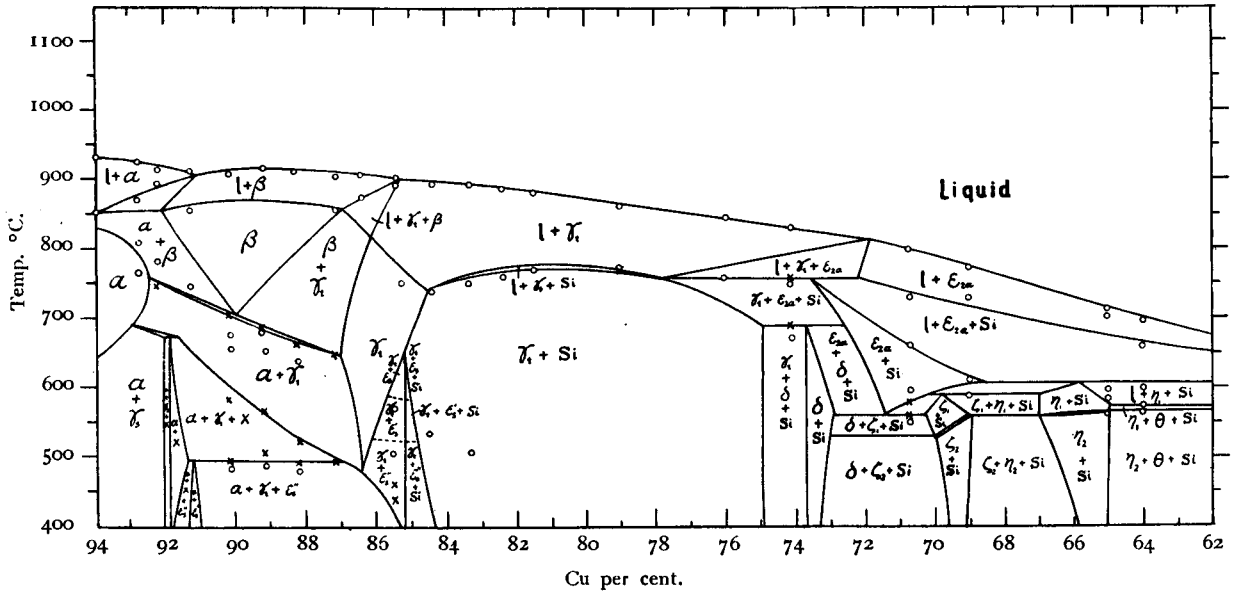

Fig. 19. TSA 10 Series. (10% Silicon).

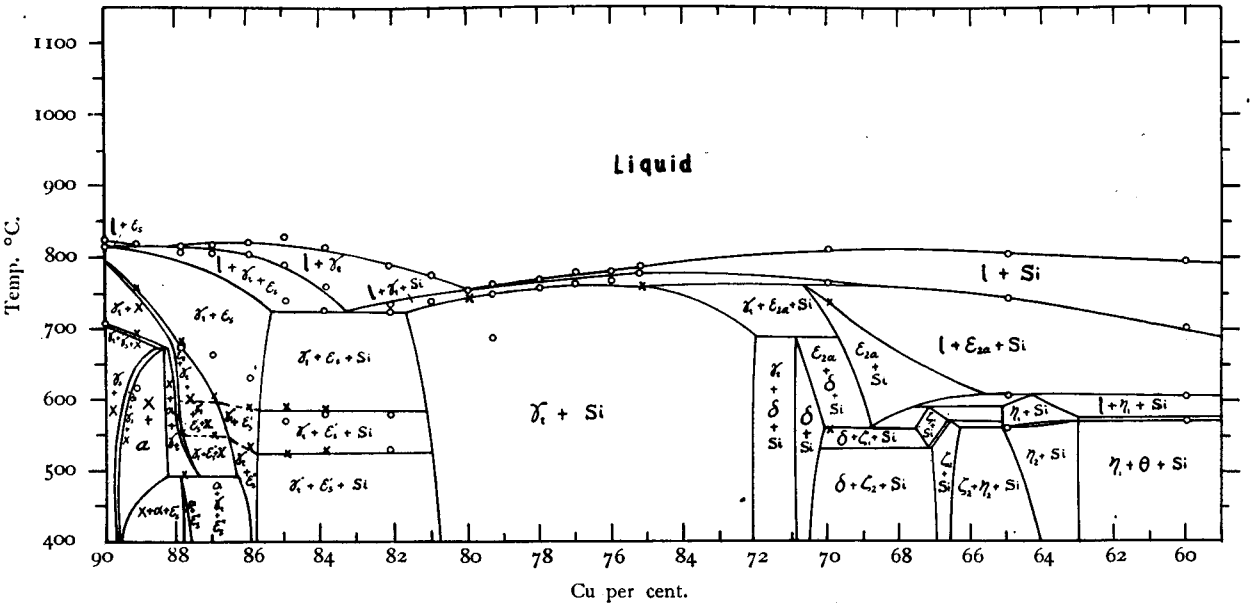

solidus of the a, $a+\beta$, β, $\beta+\gamma_a$, γ_a, $\gamma_t+\varepsilon_{1a}$, $\gamma_t+\varepsilon_{2a}$, $\varepsilon_{2a}+Si$, and η_1+Si, respectively.

In this section five invariant reactions during solidification are found. Their reacting phases are given in the following table.

Invariant line.	Temp. °C.	Reaction.
fg	910	Liquid $+\gamma_a \rightleftarrows \gamma_t + \varepsilon_{1a}$
hi	840	Liquid $+\varepsilon_{1a} \rightleftarrows \gamma_t + \varepsilon_{2a}$
jlk	760	Liquid $+\gamma_t \rightleftarrows \varepsilon_{2a}+Si$
mnp	608	Liquid $+\varepsilon_{2a} \rightleftarrows \eta_1+Si$
tru	573	Liquid $+\eta_1 \rightleftarrows \theta + Si$

Figure 16, representing constant silicon content of 2 per cent., is similar in type to Figure 15. The liquidus ABCDEFG consists of six branches: AB representing the primary separation of a; BC, primary β; CD, primary γ_a; DE, primary γ_t; EF, primary ε_{1a}; FG, primary ε_{2a}. The secondary crystallization is represented by *b*Bc, *d*Ce, *f*Dg, and *hij*E*k*F*kmnort*. These are illustrated in the following table.

Line.	Reaction.
*b*Bc	Liquid $+a \rightleftarrows \beta$
*d*Ce	Liquid $+\beta \rightleftarrows \gamma_a$
*f*Dg	Liquid $+\gamma_a \rightleftarrows \gamma_t$
hi	Liquid $\rightleftarrows \gamma_t + Si$
ij	Liquid $+\gamma_t \rightleftarrows \varepsilon_{2a}$

Fig. 20. TSA 12 Series. (12% Silicon).

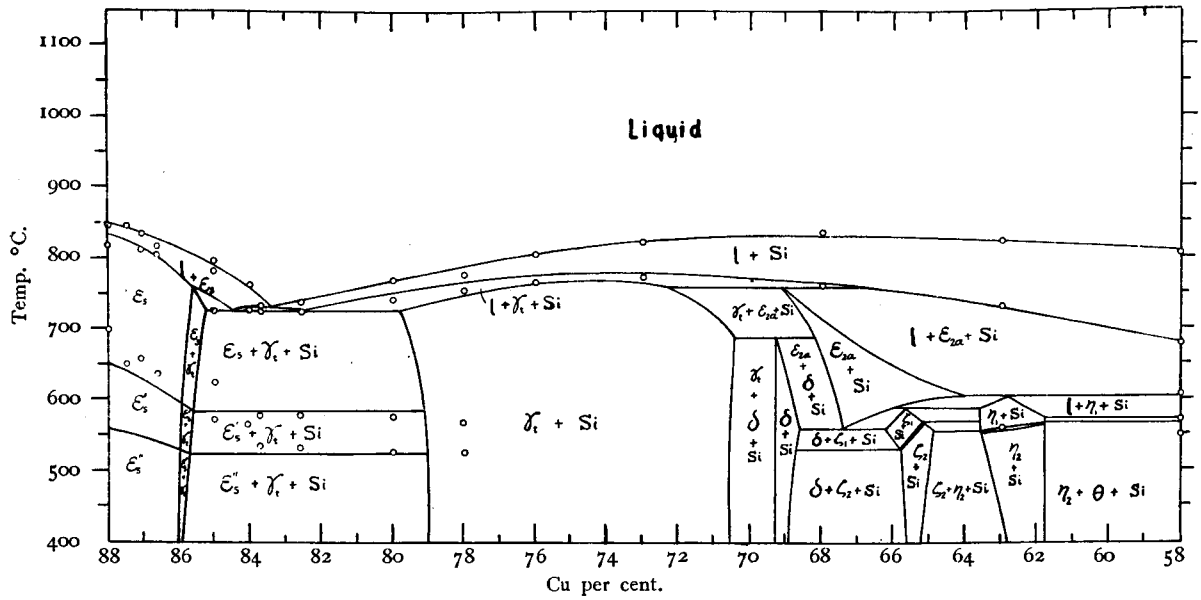

Fig. 21. TSA 20 Series. (20% Silicon).

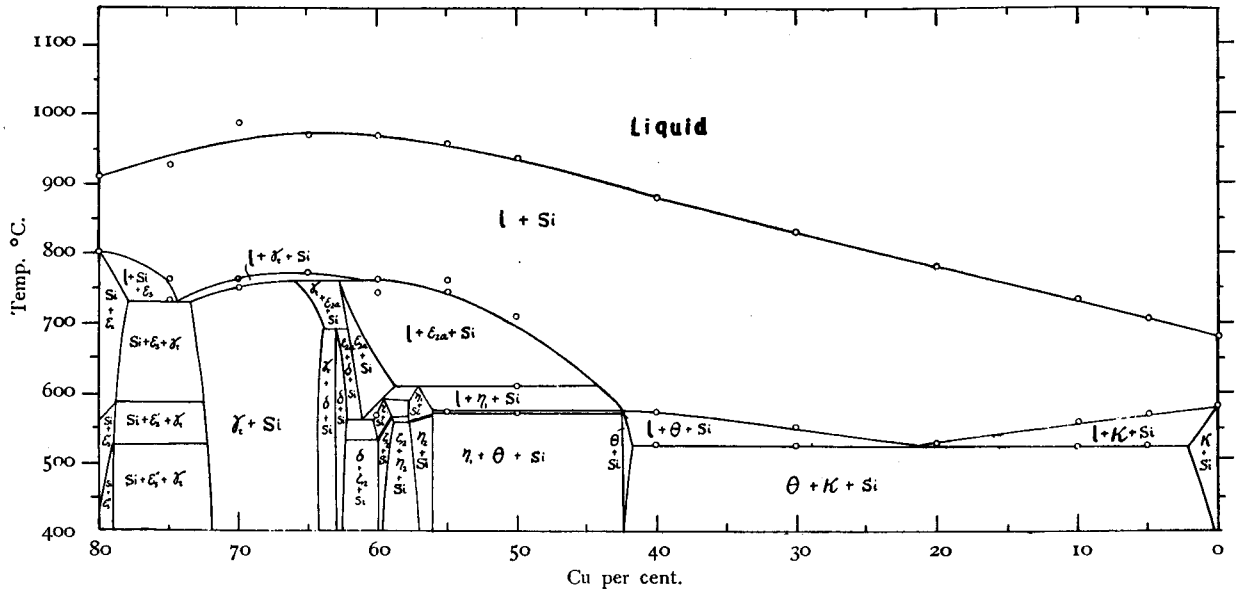

jEk	Liquid $+\gamma_t \rightleftarrows \varepsilon_{1a}$
kFk	Liquid $+\varepsilon_{1a} \rightleftarrows \varepsilon_{2a}$
km	Liquid $+\gamma_t \rightleftarrows \varepsilon_{2a}$
mn	Liquid $\rightleftarrows \varepsilon_{2a}$ + Si
nor	Liquid $+\varepsilon_{2a} \rightleftarrows \eta_1$
rt	Liquid $\rightleftarrows \eta_1$ + Si.

The solidus is represented by *abcdefghkl'ilpqst*, of which *ab*, *cd*, *ef*, and *gh* are the solidus of the α, β, γ_a, and γ_t phases, respectively. They are similar to that of the previous section, with the exception of the portion *efgh*.

The liquidus of the γ_t phase however appears in this figure in consequence of increase of silicon and the field of the primary separation of the γ_a phase diminishes.

In the sections representing alloys containing more than four per cent. of silicon the primary crystallization surface of the γ_a phase disappears due to the invariant reaction which takes place at about 980°C. As explained later, this invariant halting may be a ternary peritectic reaction

$$\text{Liquid} + \gamma_a + \beta \rightleftarrows \gamma_t.$$

The solidus of the binary complexes in this figure are summarized as follows.

Curve.	Phases.
bc	$\alpha+\beta$
de	$\beta+\gamma_a$
fg	$\gamma_a+\gamma_t$
hk'	γ_t + Si
lp	ε_{2a} + Si
qs	η_1 + Si

Fig. 22. T 1 Series. (1% Al).

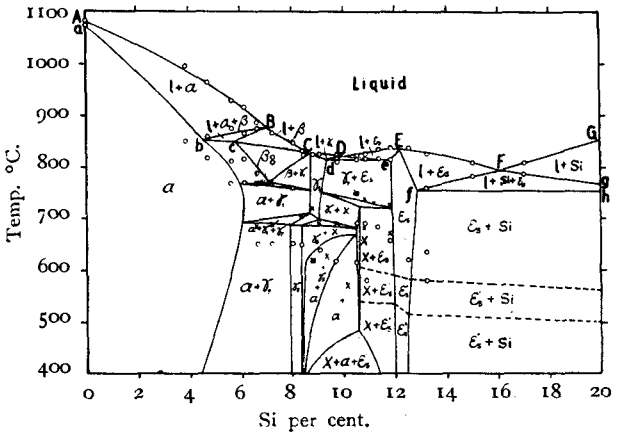

Fig. 23. T 2 Series. (2% Al).

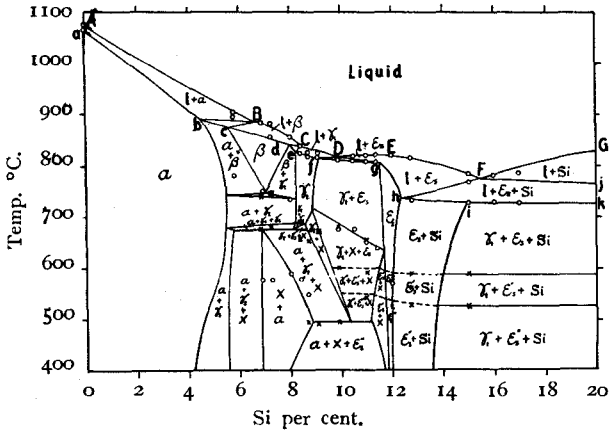

Fig. 24. T 3 Series. (3% Al).

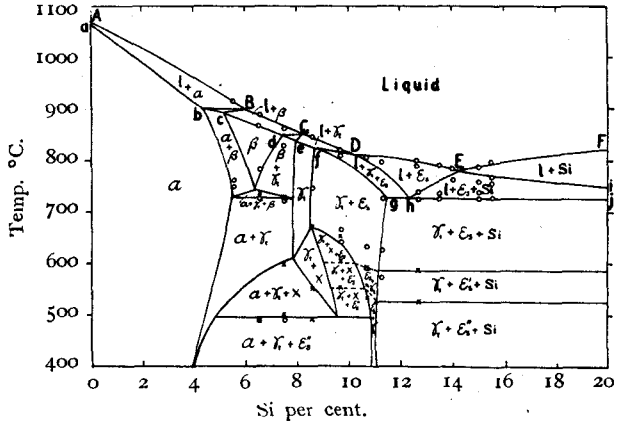

The horizontals *jk*, *l'm*, *pr*, and *st* represent the following invariant reactions:

$$\text{Liquid} + \varepsilon_{1a} \rightleftarrows \gamma_t + \varepsilon_{2a},$$
$$\text{Liquid} + \gamma_t \rightleftarrows \varepsilon_{2a} + \text{Si},$$
$$\text{Liquid} + \varepsilon_{2a} \rightleftarrows \eta_1 + \text{Si},$$
$$\text{Liquid} + \eta_1 \rightleftarrows \theta + \text{Si},$$

which are the same already described in the previous table. Concerning to the equilibrium relations, the sectional diagrams shown in Figures 17~21 are so similar to that of Figure 16, that we do not find any necessity of their explanations.

Fig. 25. T 4 Series. (4% Al).

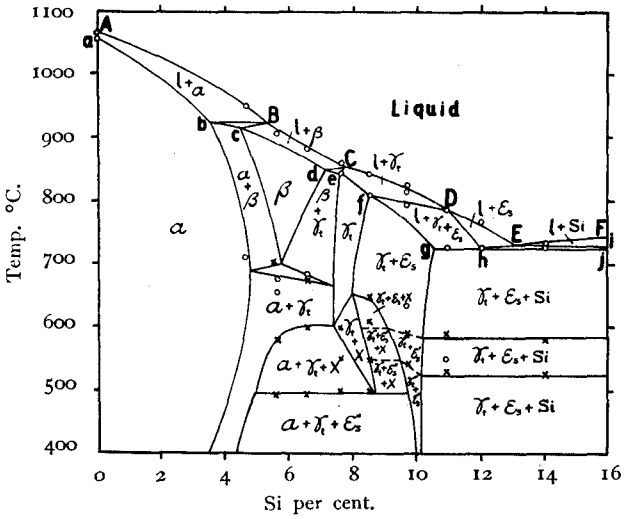

Fig. 26. T 6 Series. (6% Al).

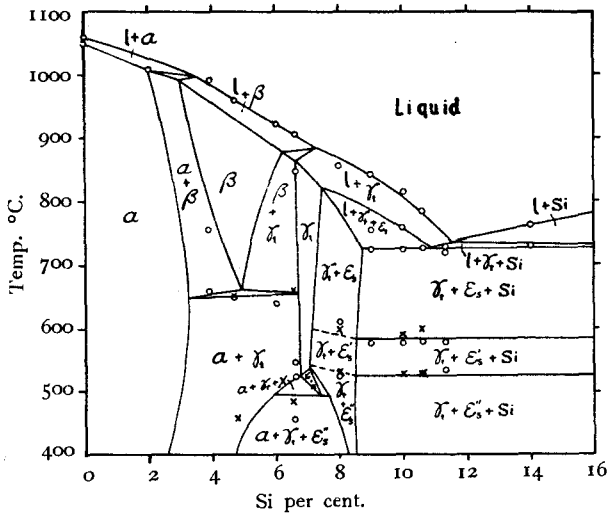

Figures 22 and 23 representing the sections of constant aluminium content of one and two per cent. respectively, may be considered together, as they are similar in type, with the exception of the horizontal *ik* in Figure 23.

The liquidus ABCDEFG consists of six or five branches: AB representing primary separation of α; BC, primary β; CD, primary γ_t; DEF, primary ε_s; FG, primary silicon.

The reactions of secondary separation in the 1 per cent. aluminium section are given by *b*B*c*, *d*D*e* and *f*F*g*, and they are summarized as follows:

Line.	Reaction.
*b*B*c*	$\text{Liquid} + \alpha \rightleftarrows \beta$
*d*D*e*	$\text{Liquid} \rightleftarrows \gamma_t + \varepsilon_s$
*f*F*g*	$\text{Liquid} \rightleftarrows \varepsilon_s + \text{Si}$

The solidus is represented by *abc*C*de*E*fh*. Of this *bc* is the solidus of the binary complex $\alpha + \beta$.

ab, *c*C, C*d*, and *e*E*f* are the solidus of the α, β, γ_t and ε_s solid solutions respectively. *de* is the solidus of the binary eutectic $\gamma_t+\varepsilon_s$, and *fh* that of the binary eutectic ε_s+Si.

The reactions of secondary separation and the solidus of the 2 per cent. aluminium are similar to that of the previous section with the exception of the portion *hik*. *hi* is the solidus of the binary eutectic ε_s+Si and the horizontal *ik* represents the following invariant reaction at about 727°C.

$$\text{Liquid} \rightleftarrows \gamma_t+\varepsilon_s+\text{Si}.$$

Sections representing alloys containing 3 and 4 per cent. aluminium (Figures 24 and 25 respectively) are slightly different from those of Figures 22–23, i.e. the phase field of ε_s in solid state does not exist in these sections.

In both sections the liquidus is represented as follows:

AB	The primary crystallization of copper (α)				
BC	,,	,,	,,	,,	β
CD	,,	,,	,,	,,	γ_t
DE	,,	,,	,,	,,	ε_s
EF	,,	,,	,,	,,	Si

*b*B*c*, *d*C*e*, *f*D and *h*E*i* represent the secondary crystallizations, Liquid + $\alpha \rightleftarrows \beta$, Liquid + $\beta \rightleftarrows \gamma_t$ Liquid $\rightleftarrows \gamma_t+\varepsilon_s$ and Liquid $\rightleftarrows \varepsilon_s$+Si, respectively.

The solidus is similar to that already described in respect to the 2 per cent. alnminium section.◎

Fig. 27.

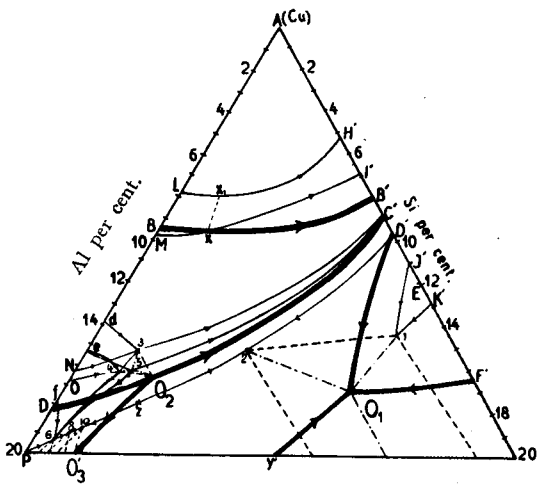

◎As in the figure 23, the horizontal *ghj* represents the solidus due to the ternary eutectic reaction at O_1 as shown in Figure 27.

Summarizing the results of thermal analysis during solidification, we obtained the equilibrium diagrams as shown in Figures 27 and 28. In these figures, fields of the primary separation of α, β, γ_α, γ_t, ε_s, $\varepsilon_{1\alpha}$, $\varepsilon_{2\alpha}$ and Si are respectively represented by ABB′, BB′C′O_2D, DO_2O_3E, $O_2O_3O_5yO_1$D′C′, D′O_1F′, EO_3O_4F, FO_4O_5 and F′O_1O_5. The lines of the univariant reactions in these alloys are summarized in Table 22.△

Fig. 28.

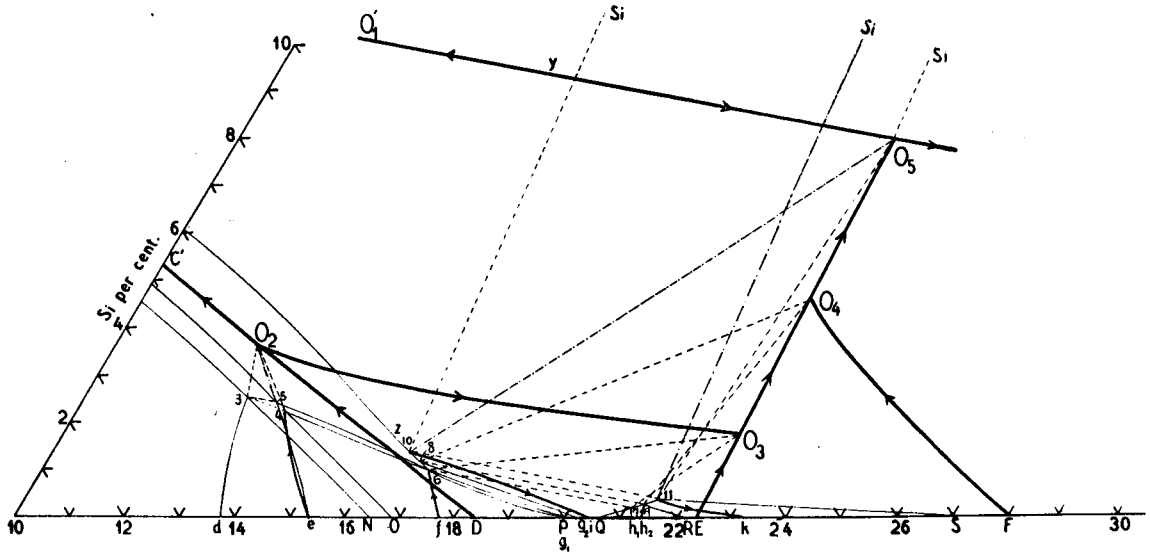

△ As explained in Table 22, the reaction along the curve BB′ is transformed at a point x from the binary eutectic reaction, Liquid $\rightleftarrows \alpha+\beta$, to the peritectic reaction, Liquid+$\alpha \rightleftarrows \beta$, and finally it coincides with the peritectic point of the binary system of copper and silicon. Similarly the peritectic curve O_2C′, Liquid+$\gamma_t \rightleftarrows \beta$, proceeds from O_2 to C′ on the Cu-Si side. The eutectic curve O_1O_5 has a maximum point y at about 780°C.

Thus we found five invariant points, O_1, O_2, O_3, O_4, O_5, on the liquidus surface, whose composition and reacting phases are given in Table 23.

Table 22.

Univariant reaction lines on Liquidus.

Reaction curve.	Reaction.
Binary eutectic curve, Bx	Liquid$\rightleftarrows\alpha(Lx_1)+\beta(M\tau)$
„ peritectic curve, xB′	„ $+\alpha(x_1H')\rightleftarrows\beta(xI')$
„ „ „ DO_2	„ $+\gamma_\alpha(O4)\rightleftarrows\beta(N3)$
„ „ „ O_2C'	„ $+\gamma_\varepsilon(5C')\rightleftarrows\beta(3C')$
„ „ „ O_2O_3	„ $+\gamma_\alpha(46)\rightleftarrows\gamma_\varepsilon(56)$
„ „ „ EO_3	„ $+\gamma_\alpha(P6)\rightleftarrows\varepsilon_{1\alpha}(Q7)$
„ „ „ O_3O_4	„ $+\gamma_\varepsilon(68)\rightleftarrows\varepsilon_{1\alpha}(79)$
„ „ „ FO_4	„ $+\varepsilon_{1\alpha}(R9)\rightleftarrows\varepsilon_{2\alpha}(R9)$
„ „ „ O_4O_5	„ $+\gamma_\varepsilon(810)\rightleftarrows\varepsilon_{2\alpha}(911)$
„ eutectic „ yO_5	„ $\rightleftarrows\gamma_\varepsilon(\varepsilon10)+Si$
„ „ „ yO_1	„ $\rightleftarrows\gamma_\varepsilon(22)+Si$
„ „ „ $D'O_1$	„ $\rightleftarrows\gamma_\varepsilon(D'2)+\varepsilon_\delta(J'1)$
„ „ „ $F'O_1$	„ $\rightleftarrows\varepsilon_\delta(K'1)+Si$

Table 23.

Point	Composition. Cu%	Al%	Si%	Temperature °C	Reaction.	The range of reaction.
O_1	83	5.5	11.5	727	Liquid$\rightleftarrows\gamma_\varepsilon+\varepsilon_\delta+Si$	**1** Si **2**
O_2	84	12.5	3.5	980	„ $+\gamma_\alpha+\beta\rightleftarrows\gamma_\varepsilon$	**3** O_2 **4**
O_3	76	22.2	1.8	910	„ $+\gamma_\alpha\rightleftarrows\gamma_\varepsilon+\varepsilon_{1\alpha}$	**6** O_3 **7**
O_4	73.5	22.0	4.5	840	„ $+\varepsilon_{1\alpha}\rightleftarrows\varepsilon_{2\alpha}+\gamma_\varepsilon$	**8** O_4 **9**
O_5	70.0	22.0	8.0	760	„ $+\gamma_\varepsilon\rightleftarrows\varepsilon_{2\alpha}+Si$	**10** SiO_5 **11**

Among these points, the invariant reaction O_2 is not shown in sectional diagrams but its existence has been ascertained especially on the alloys near the composition of O_2 by thermal analysis as shown in Table 21.

Table 24.

Results of Thermal Analysis in Solid State.

No.	Arrest temperatures. °C. On Heating.			On Cooling.	
TSA 109	550			530	
„ 111	555			550	516
„ 113	561			520	514
„ 114	555			518	
„ 115	885				
„ 118	745	780			
„ 119	735	760			
„ 120	735	762			
„ 121	690	760			
„ 122	575	692	730		
„ 125	550	586	630		
„ 128	570	590	605		
„ 130	568	573	596	610	
„ 133	568	573	605		
„ 135	568	571			
„ 208	none				
„ 209*	553			520	
„ 210	560			528	
„ 211	562				526
„ 212	562				515
„ 216	770				
„ 217	768				
„ 220	730	750			
„ 221	686	744			
„ 222	622	730	758		
„ 223	530	560	590		
„ 225	570	589	610	646	
„ 227	550	570			
„ 229	570	574			
„ 231	570	575			
„ 232	568	575			
„ 405	none				
„ 406	650	749			630
„ 407	618				600
„ 408	612				600
„ 409	620				600
„ 410	605				598
„ 411	600				
„ 413	773				
„ 415	760				
„ 416	760				
„ 420	690	760			
„ 422	560	700			
„ 424	570	590	638		
„ 426	580	590	605		
„ 430	569	575			
„ 602	746				
„ 604	493	580	705		
„ 605	510	570	686		658 500
„ 606	490	520	664		
„ 607	490	648			
„ 608	440	460			
„ 615	770				
„ 620	689	760			
„ 625	560	580			
„ 1001	692	756		688	748
„ 1002	495	550	600	680	
„ 1003	552	606	656		
„ 1004	531	580			
„ 1005	525	585			
„ 1006	527	581			
„ 1010	743				
„ 1015	761				
„ 1020	560	740			
T 17	683	770			
„ 17.5	688	770			
„ 18.5	708				
„ 19	620	720			
„ 19.5	690	752			748
„ 110	685	548			
„ 110.5	682	750			
„ 111	683	740			
„ 111.5	735				
TSA 1201	670	730			
T 27	676	740			

„	27.5	680	748			740	636
„	28.5	658				608	
„	29	493	550	610	650	643	
„	29.5	490	550	675			
TSA	1002	495	550	600	680		
T	211	540	590	653			
TSA	1202	526	582				
T	213	529	564	590			
„	215	524	588				
„	217	524	584				
„	37	680	730			726	
„	38	500	595	724		718	
„	39	491	550	606	670		
„	310	552	606	656			
„	311	532	562	590			
„	313	524	584				
„	47	493	600	672		638	
„	48	500	550	600			
„	49	500	548	610	650		
„	411	532	592				
„	414	526	580				
„	605	460	655				
„	607	480	662				
„	608	530	600				
„	609	526	582				
„	611	528	562	590			
TSA	1206	528	564	594			
„	807	538	560	588			
„	708	515	550	578			
„	1010	520	560				

* Composition is given as charged (Cu 89%, Si 2%, Al 9%).

(2) The Study of Solid Transformation.

For the determination of changes in the solid state, specimens were annealed and tested in the same way as has been described in the previous research.*

The results of the experiments are summarized in Table 24. They are also plotted in the constitutional sections as shown in Figures 15 to 26, where they are represented by the symbol of a cross ×.

Figures 29 (a) and (b) show the equilibrium relation in the solid state of the alloys near the Cu-Si side; the former is the equilibrium diagram obtained by the results of the present experiments, while the latter is a magnified diagram for explanation of the relation between the α, γ_s, γ_t, X and ε_s phases.

The binary complex lines showing the univariant reactions in Figure 29 together with those of Figure 28 are summarized as follows.

As shown in the figures, both the β phases of the Cu-Al and Cu-Si systems are completely soluble in all proportion, and the eutectoid curve $b'y'b$ proceeds from b' on the Cu-Si system to b on the Cu-Al side. A minimum point y' was found to exist on this curve and its temperature was determined to be about 550° and 515°C from heating and cooling curves respectively; its composition being about 11 per cent. of aluminium, 1-2 per cent. of silicon and the rest of copper. x' and z' denote the conjugate phases of α and γ_t with β (y') phase at this minimum point.

The temperature of the binary eutectoid reaction of the Cu-Al system, $\gamma_a \rightleftarrows \gamma_t + \beta$, rises with the addition of silicon as shown by the curve e_4, and finally reaches the invariant halting temperature at about 980°C. At this temperature the ternary peritectic reaction, Liquid + $\gamma_a + \beta \rightleftarrows \gamma_t$,

Fig. 29–a.

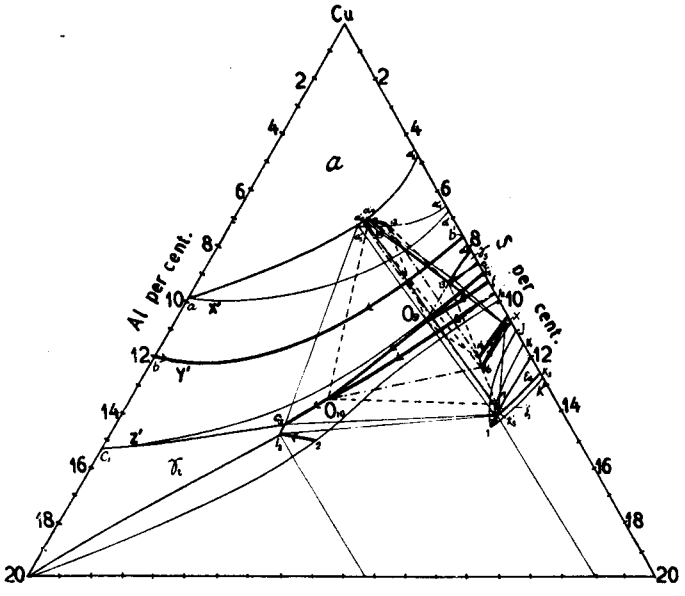

Fig. 29–b.

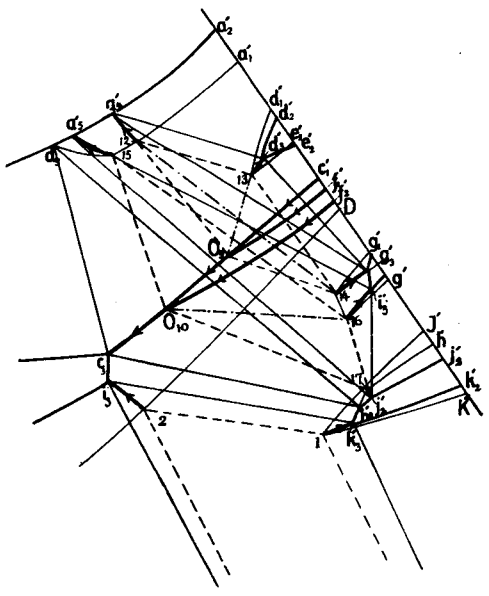

* Memoirs of the College of Engineering, Kyoto Imp. Univ., Vol. VIII, No. 2. P. 75.

Table 25.

Binary Complex Lines in Solid State.

Reaction curve.	Reaction.
Binary peritectoid curve, $f_2'O_{10}$	$\gamma_t(f_2'O_{10})+\varepsilon_s(h'17)\rightleftarrows X(g'16)$
„ eutectoid curve, $f_1'O_9$	$\gamma_t(f_1'O_9)\rightleftarrows\gamma_s(e_1'13)+X(g_1'14)$
„ „ „ O_9O_{10}	$\gamma_t(O_9O_{10})\rightleftarrows\alpha(12\cdot15)+X(14\cdot16)$
„ peritectoid curve, $c_1'O_9$	$\gamma_t(c_1'O_9)+\alpha(a_1'12)\rightleftarrows\gamma_s(d_1'13)$
„ eutectoid curve, $O_{10}c_3$	$\gamma_t(O_{10}c_3)\rightleftarrows\alpha(15a_3')+\varepsilon_s''(17h_3')$
„ „ „ $b'y'b$	$\beta(b'y'b)\rightleftarrows\alpha(a'x'a)+\gamma_t(c'_2'c_1)$
„ „ „ $1k_3'$	$\gamma_t(2i_3)\swarrow^{\varepsilon_s(1k_3')}\searrow Si$
„ „ „ $2i_3$	
„ „ „ $12a_4'$	$\alpha(12a_4')\swarrow^{\gamma_s(13d_3')}\searrow X(14g_3')$
„ „ „ $13d_3'$	
„ „ „ $14g_3'$	
„ „ „ $15a_5'$	$\alpha(15a_5')\swarrow^{X(16i_3')}\searrow\varepsilon_s''(17j_2')$
„ „ „ $16i_3'$	
„ „ „ $17j_2'$	
„ „ „ $e4$ (Fig. 28)	$\gamma_a(e4)\rightleftarrows\gamma_t(e5)+\beta(d3)$
„ peritectoid curve, $f6$ (Fig. 28)	$\gamma_a(f6)+\varepsilon_{1a}(h17)\rightleftarrows\gamma_t(g_16)$
„ eutectoid curve, $10i$	$\gamma_t(10i)\swarrow^{\varepsilon_{2a}(11k)}\searrow Si$
„ „ „ $11k$ (Fig. 28)	

occurs as previously described.

Similarly the binary peritectoid curve f_6, $\gamma_a+\varepsilon_{1a}\rightleftarrows\gamma_t$, proceeds from f of the Cu-Al system at 873 C° to *6* on the peritecto-eutectic reaction, Liquid $+\gamma_a\rightleftarrows\gamma_t+\varepsilon_{1a}$, at about 910°C. At *6* point the γ_a phase coincides with the γ_t phase. When the alloys in the field *10. 11.* Si have just crystallized, they consist of γ_t, ε_{2a} and silicon. These γ_t and ε_{2a} phases change their composition along *10i* and *11k*, separating $\varepsilon_{2a}+Si$ and γ_t+Si respectively.

The constituents of the δ, ε_{1a}, ε_{2a}, ζ_1, ζ_2, η_1 and η_2 of the Cu-Al system form solid solutions with silicon, whose solubility might be less than 0.5 per cent. And the binary invariant reactions of the above mentioned phases are hardly affected by the addition of silicon. In other word, in the ternary system these invariant reactions; $\gamma_t+\varepsilon_{2a}\rightleftarrows\delta+Si$, $\varepsilon_{2a}\rightleftarrows\delta+\zeta_1+Si$, $\zeta_1\rightleftarrows\delta+\zeta_2+Si$, $\varepsilon_{2a}+\eta_1\rightleftarrows\zeta_1+Si$, $\zeta_1+\eta_1\rightleftarrows\zeta_2+Si$, and two ternary polymorphic changes due to the $\eta_1\rightleftarrows\eta_2$ phases, take place at the same temperatures as that of the binary Cu-Al system, as observed in thermal analysis shown in Table 24 and microscopic examination. These are summarized as follows:

Reaction.	Temp. °C.
Ternary peritecto-eutectoid reaction $\gamma_t+\varepsilon_{2a}\rightleftarrows\delta+Si$	686
„ eutectoid reaction $\varepsilon_{2a}\rightleftarrows\delta+\zeta_1+Si$	560
„ eutectoid reaction $\zeta_1\rightleftarrows\zeta_2+\delta+Si$	530
„ peritecto-eutectoid reaction $\varepsilon_{2a}+\eta_1\rightleftarrows\zeta_1+Si$	590
„ peritecto-eutectoid reaction $\zeta_1+\eta_1\rightleftarrows\zeta_2+Si$	570
„ polymorphic reactoin $\eta_1+\zeta_2\rightleftarrows\eta_2+Si$	560
„ polymorphic reactoin $\eta_1+\theta\rightleftarrows\eta_2+Si$	563

The univariant reaction curves $c_1'O_9$ and $f_1'O_9$ intersecting at O_9, and that of O_9O_{10} and f_2' O_{10} at O_{10}, there occur two invariant reactions as shown in the following table.

Table 26.

Invariant Points in the Solid State.

Point.	Temp. °C.	Composition. %	Reaction.
O_9	675	Al≒2.5, Si≒8.0	Peritecto-eutectoid reaction. $\gamma_t(O_9)+\gamma_s(13)\rightleftarrows\alpha(12)+X(14)$
O_{10}	495	Al≒7.5, Si≒6.3	Peritecto-eutectoid reaction. $\gamma_t(O_{10})+X(16)\rightleftarrows\alpha(15)+\varepsilon_s''(17)$

The alloys containing the ε_s phase show thermal changes due to the polymorphic transformations of $\varepsilon_s\rightleftarrows\varepsilon_s'$ and $\varepsilon_s'\rightleftarrows\varepsilon_s''$. Ternary invariant reactions due to the above transformations are to be seen in Figures 23–26 and are summarized as follows.

Reaction.	Temp. °C.
$\gamma_t+\varepsilon_s\rightleftarrows\varepsilon_s'+X$	600
$\gamma_t+\varepsilon_s'\rightleftarrows\varepsilon_s''+X$	550
$\gamma_t+\varepsilon_s\rightleftarrows\varepsilon_s'+Si$	585
$\gamma_t+\varepsilon_s'\rightleftarrows\varepsilon_s''+Si$	525

B. Microscopic Examination.

The microstructures of alloys were carefully observed with reference to the results of the thermal analysis, the sectional diagrams being thus determined. As etching reagents for microscopic observation, a cupric chloride solution, an Iodine solution, an alcoholic ferric chloride solution and a potassium bichromate solution (saturated $K_2C_{12}O_7$ solution + 10% H_2SO_4 + 2% NaCl.) were used.

With both the cupric chloride and Iodine solutions the phases of the Cu-Al side are easily distinguished from each other, as was found in the previous investigation. On the other hand, for the alloys of the Cu-Si series, good results are obtained by using the alcoholic ferric chloride solution. A better result can also be obtained in etching the alloys consisting the γ_s, γ_t, X and ε_s phases in a bichromate solution. The etching surface of alloys containing the X and ε_s phases gradually turn red in colour in the course of time, hence the existence of these phases is easily ascertained. The specimens in the following tables were examined in accordance with these recommendations.

1) The microstructures of alloys containing a constant silicon content of 1–4 per cent.

The phases obtained from quenching experiments are given in Table 27.

Table 27.

No.	Quenching Temp. °C.	Heating Time. (hours)	Phases.
TSA 1 Series.			
TSA 107	510	16	α
„	800	2	α
„ 109	510	16	α+γ_t
„	650	6	α+β
„	800	2	β
„ 110	510	16	α+γ_t
„	650	6	β+α
„	800	2	β
„ 111	510	16	α+γ_t
„	650	6	β
„	800	2	β
„ 112	510	16	α+γ_t
„	650	6	β+γ_t
„	800	2	β
„ 113	510	16	γ_t+α
„	650	6	γ_t+β
„	800	2	γ_t+β
„	900	2	β
„ 114	510	16	γ_t+α
„	800	2	γ_t+β
„	860	2	γ_t+β
„	900	2	γ_t+β
„	940	2	γ_a+β
„ 115	510	16	γ_t
„	650	6	γ_t
„	800	2	γ_t
„	850	8	γ_t
„	900	2	γ_a
„	920	2	γ_a
„	960	4	γ_a
„ 116	510	16	γ_t
„	650	6	γ_t
„	800	2	γ_t
„	850	8	γ_t
„	900	2	γ_t
„	920	2	γ_a
„ 117	510	16	γ_t+Si
„	650	6	γ_t+Si
„	800	2	γ_t
„	860	4	γ_t
„	870	1	γ_t+Melt
„ 118	510	16	γ_t+Si
„	650	6	γ_t+Si
„	720	20	γ_t+Si
„ 119	510	6	γ_t+Si
„	650	6	γ_t+Si
„	750	2	γ_t+ε_{2a}+Si
„ 120	510	6	γ_t+δ+Si
„	650	6	γ_t+Si
„	750	2	γ_t+ε_{2a}+Si
„ 121	510	6	ζ+Si
„	650	6	ζ+Si
„	670	6	δ+Si
„	695	2	γ_t+ε_{2a}+Si
„	730	2	γ_t+ε_{2a}+Si
„ 122	500	20	δ+ζ_2+Si
„	570	20	δ+ε_{2a}+Si
„	600	20	δ+ε_{2a}+Si
„	650	6	δ+ε_{2a}+Si
„	720	8	ε_{2a}+Si
„ 123	500	20	δ+ζ_2+Si
„	550	18	δ+ζ_1+Si
„	600	20	ε_{2a}+Si
„ 124	550	18	ζ_1+δ+Si
„	600	20	ε_{2a}+Si
„	680	2	ε_{2a}+Si+Melt
„ 125	550	18	ζ_1+Si
„	600	20	ε_{2a}+Si
„ 126	550	18	ζ_1+Si
„	600	20	ε_{2a}+Si
„ 127	550	18	ζ_2+η_2+Si
„	600	20	ε_{2a}+η_1+Si
„ 128	550	18	η_2+Si
„	570	2	η_1+Si
„	590	2	η_1+Si
„ 130	550	18	η_2+θ+Si
„	580	2	η_1+Si+Melt
„ 132	550	18	η_2+θ+Si
„ 135	550	18	η_2+θ+Si
TSA 2 Series.			
TSA 206	500	20	α
„	800	4	α
„ 208	500	20	α+γ_t
„	800	4	α+β
„ 210	500	20	α+γ_t
„	700	2	β
„	800	4	β
„ 211	500	20	α+γ_t
„	700	2	β+γ_t
„	800	4	β
„ 212	500	20	γ_t+α
„	700	2	γ_t+β
„	800	4	γ_t+β
„	900	2	γ_t+β
„ 213	500	20	γ_t
„	700	2	γ_t
„	800	4	γ_t
„ 214	500	20	γ_t
„	700	2	γ_t
„	800	4	γ_t
„ 215	500	20	almost homogeneous γ_t phase
„	700	2	„ „ „ „
„	800	4	γ_t+Melt
„ 216	500	20	γ_t+Si
„	700	2	γ_t+Si
„	806	4	γ_t+Si+Melt
„ 217	500	20	γ_t+Si

"	700	2	γ_t+Si
"	750	4	γ_t+Si
" 218	500	20	γ_t+Si
"	700	2	γ_t+Si
"	750	4	γ_t+Si
" 219	500	20	γ_t+Si
"	700	2	γ_t+Si
"	750	4	γ_t+ε_{2a}+Si
" 220	500	20	γ_t+Si
"	700	2	γ_t+Si
"	730	6	γ_t+ε_{2a}+Si
" 221	500	20	δ+Si
"	600	40	δ+Si
"	670	6	δ+Si
"	700	2	γ_t+ε_{2a}+Si
"	730	6	γ_t+ε_{2a}+Si
" 222	500	20	δ+ζ_2+Si
"	600	40	δ+ε_{2a}+Si
"	730	6	ε_{2a}+Si
" 223	500	20	δ+ζ_2+Si
"	600	40	ε_{2a}+Si
"	730	6	ε_{2a}+Si+Melt
" 224	500	20	ζ_2+δ+Si
"	600	40	ε_{2a}+Si
"	660	2	ε_{2a}+Si
" 225	500	20	ζ_2+Si
"	600	40	ε_{2a}+Si
"	660	2	ε_{2a}+Si+Melt
" 227	500	20	η_2+ζ_2+Si
"	600	40	ε_{2a}+η_1+Si
" 229	500	20	η_2+Si
"	570	2	η_1+Si
"	580	1	η_1+Si+Melt
" 231	500	20	η_2+θ+Si

TSA 4 Series.

TSA 405	550	70	almost homogeneous α phase
"	700	2	α+β
"	800	4	α+β
" 406	550	70	α+γ_t
"	700	2	α+β
"	800	4	almost β phase
"	930	0.5	β+Melt
" 407	550	70	α+γ_t
"	700	2	almost β phase
"	800	4	β
" 408	550	70	α+γ_t
"	700	2	β
"	800	4	β
" 409	500	70	γ_t+α
"	700	2	β+γ_t
"	800	4	almost β phase
" 410	500	70	γ_t+α
"	700	2	γ_t+β
"	800	4	β+γ_t
"	860	1	β
"	920	1	β+Melt
" 411	500	70	γ_t+a little α
"	700	2	γ_t+β
"	800	4	γ_t+β
" 412	500	70	γ_t
"	700	2	γ_t
"	800	4	γ_t
"	860	0.5	γ_t+Melt
" 413	500	70	γ_t+Si
"	800	4	γ_t+Melt
" 414	600	120	γ_t+Si
" 415	600	120	γ_t+Si
" 418	600	120	γ_t+Si
"	730	8	γ_t+Si
" 419	600	120	γ_t+Si
" 420	600	120	δ+Si
"	730	8	γ_t+ε_{2a}+Si
" 421	600	120	δ+Si
"	650	6	δ+ε_{2a}+Si
"	730	8	δ+ε_{2a}+Si
" 422	600	120	δ+ε_{2a}+Si
"	650	6	δ+ε_{2a}+Si
" 423	500	120	δ+ζ_2+Si
"	600	120	ε_{2a}+Si
" 424	500	120	ζ_2+Si
"	600	120	ε_{2a}+Si
" 425	500	120	ζ_2+Si
" 426	500	120	ζ_2+η_2+Si
"	600	120	ε_{2a}+η_1+Si
" 428	500	120	η_2+Si
"	600	120	η_2+Si+Melt
" 430	500	120	η_2+θ+Si

The changes of the microstructure of the alloys which take place below the solidus are almost similar in the three sections considered above. One section will, therefore, be described in detail, i.e. 1 per cent. of silicon.

The ranges of each of the β, and γ_t phases gradually decrease on the addition of silicon; for example the existing field of the latest phase extends from 84.7 to 82.2 per cent. of copper in one per cent. silicon section, and from 84.8 to 83.8 per cent. of copper in four per cent. silicon section at about 500°C. Photograph 1 shows a microstructure of the alloy TSA 412 (containing about 4 per cent. of silicon and about 12 per cent. of aluminium) quenched at 500°C. after heating for 70 hours at that temperature. As seen in the figure, it consists only of a solid solution of the γ_t phase. Photograph 2 illustrates the microstructure of the alloy containing 82.43 per cent. of copper and 1.01 per cent. of silicon, quenched from 920°C in water, and it shows that there exist large crystals of the γ_a phase. Even if the same alloy is quenched at 850°C in water, the structure is homogeneous as shown in Photograph 3, but this is γ_t. It was very difficult to distinguish the struc-

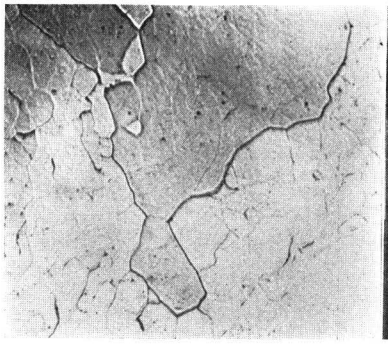

(1) TSA 412 (84.28% Cu, 4.00% Si)
Quenched at 500°C.
γ_t. × 100.

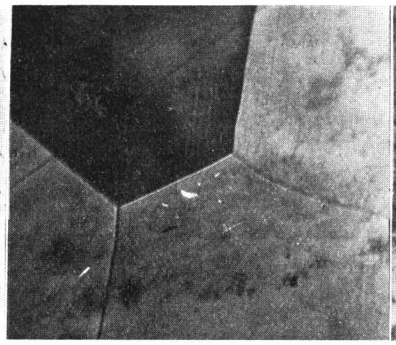

(2) TSA 116 (82.43% Cu, 1.01% Si)
Quenched at 920°C.
γ_a. × 100.

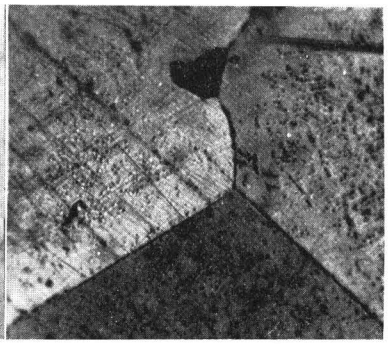

(3) TSA 116 (82.43% Cu, 1.01% Si)
Quenched at 850°C.
γ_t. × 100.

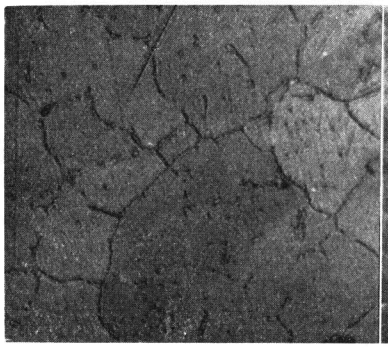

(4) TSA 118 (80.38% Cu, Si 1.02%)
Quenched at 510°C.
γ_t+Si. × 100.

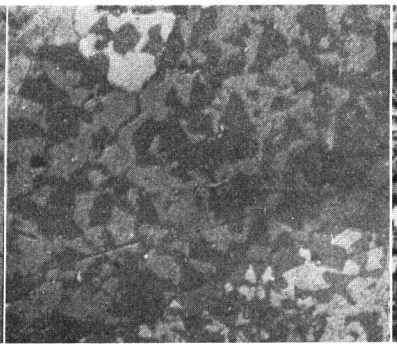

(5) TSA 120 (78.82% Cu, 0 99% Si)
Quenched at 510°C.
$\gamma_t+\delta$+Si. × 100.

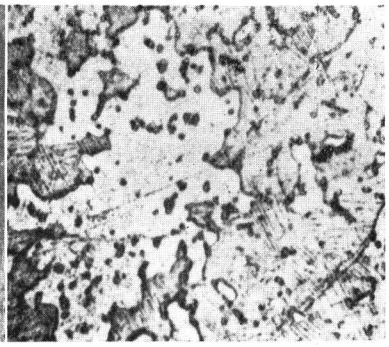

(6) TSA 121 (78.1% Cu, 1.02% Si)
Quenched at 670°C.
δ+Si. × 100.

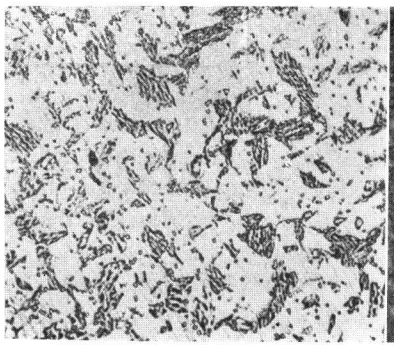

(7) TSA 121 (78.1% Cu, 1.02% Si)
Quenched at 730°C.
$\gamma_t+\varepsilon_{2a}$+Si. × 100.

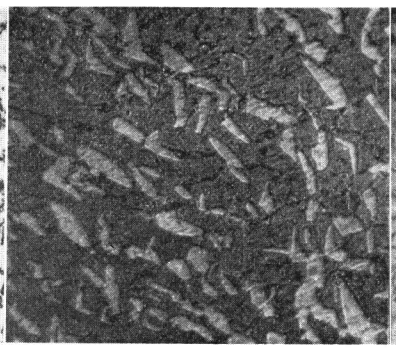

(8) TSA 122 (76.78% Cu, 1.14% Si)
Quenched at 600°C.
$\delta+\varepsilon_{2a}$+Si. × 100.

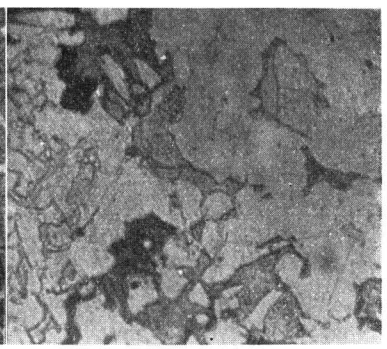

(9) T 422 (74.0% Cu, 4.0% Si)
Quenched at 600°C.
$\delta+\varepsilon_{2a}$+Si. × 150.

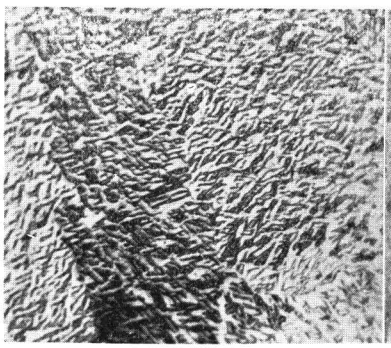

(10) TSA 123 (75.86% Cu, 1.27% Si)
Quenched at 550°C.
$\delta+\zeta_1$+Si. × 150.

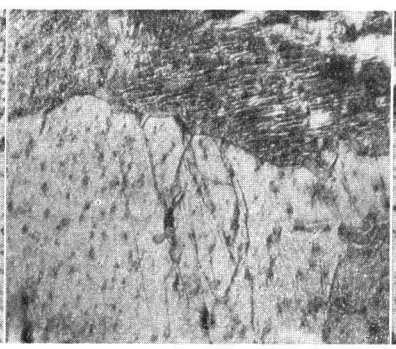

(11) TSA 126 (73.11% Cu, 1.04% Si)
Quenched at 600°C.
Decomposed ε_{2a}+Si. × 100.

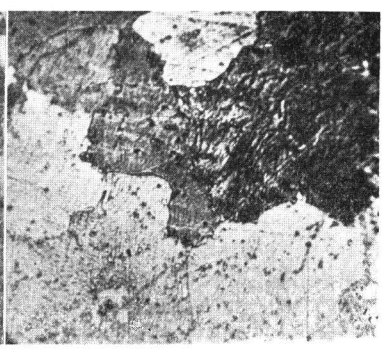

(12) TSA 124 (75.12% Cu, 1.30% Si)
Quenched at 600°C.
ε_{2a}+Si. × 100.

tures between the γ_a and γ_t phases as illustrated in the previous investigation of Cu-Al system. The present writer could not find the two-phase field $\gamma_a + \varepsilon_{1a}$ from the microstructures of the quenched specimens even in the section of TSA 1 series. Photographs 4 and 5, under a magnification of 100 diameters, show the structures of the alloys TSA 118 and TSA 120, containing about 1 per cent. of silicon and 80.38 and 78.82 per cent. of copper respectively.

The alloy TSA 118 is seen to consist only of γ_t and Si, while the alloy TSA 120 consists of γ_t, δ and Si. In these photographs small silicon crystals are clearly found in the boundary of the large γ_t crystals. The phase field consisting of γ_t, ε_{2a} and Si has been also determined from the microscopical examination of quenched specimens. Photograph 7 of a 78.1 per cent. of copper and 1.02 per cent. of silicon alloy quenched from 730°C. in water shows such a structure of a three-phase field. The same alloy quenched from below the temperature of the invariant reaction, $\gamma_t + \varepsilon_{2a} \rightleftarrows \delta + \mathrm{Si}$, shows the structure of the two-phase field consisting of $\delta + \mathrm{Si}$, as shown in Photograph 6.

Photograph 8 shows the microstructure of an alloy TSA 122 containing 76.78 per cent. of copper and 1.14 per cent. of silicon quenched at 600°C. in water. In this photograph the δ crystals exist in the ground of the decomposed ε_{2a} phase and a small amount of silicon is seen to be present.

The alloy TSA 422 containing 74.0 per cent. of copper and 4.0 per cent. silicon shows a similar structure to that in the above photograph, but a large amount of the silicon crystals is seen in the form of fine needles and rounded particles. Photograph 9 shows such a microstructure of the alloy TSA 422 quenched at 600°C. after heating for 120 hours at that temperature. In this figure the dark etching constituents are the decomposed ε_{2a} phase and silicon is present as a half- tone colour, and these exist in the ground of the δ phase. Photograph 10 is the photo-micrograph of the TSA 123 alloy containing 75.86 per cent. of copper and 1.27 per cent. of silicon, quenched at 550°C in water. In it the eutectoid structure is seen to consist of $\delta + \zeta_1$ plus a very little silicon due to the invariant reaction, $\varepsilon_{2a} \rightleftarrows \delta + \zeta_1 + \mathrm{Si}$. The ε_{2a} crystal has little solubility with silicon, and it is shown always in decomposed structure to be the same as in the binary Cu-Al system. This is evident in photographs 11 and 12, which are the microstructures of decomposed ε_{2a} crystals plus Si in the alloys containing 73.11 and 75.12 per cent. of copper respectively and about 1 per cent. of silicon.

In photograph 12, under a magnification of 100 diameters, the ε_{2a} phase appears uniform, though examination under high powers shows that each crystal shows in the observation is really a mass of two constituents in a very finely divided state.

The solubilities of silicon in the ζ and η phases are also very small. It is shown in photographs 13 to 15, under a magnification of 150 diameters.

Photograph 13 is a microstructure of an alloy containing 73.88 per cent. of copper and 1.19 per cent. of silicon quenched at 550°C. in water. It shows some amount of silicon existing in the boundary of the twinned ζ_1 phase. These silicon crystals are found more definitely when silicon is added.

The existing field of the ζ_2 and η_2 phases in the binary Cu-Al system is also determined by the present investigation. In photograph 14, the structure of the $\zeta_2 + \eta_2$ phases coexisting with silicon is shown. Photograph 15 of a 70.73 per cent. of copper and 1.26 per cent. of silicon alloy quenched at 570°C. in water shows a two-phase field of $\eta_1 +$ Si, in which silicon is seen in angular form.

Photograph 16 illustrates a microstructure of specimen TSA 420 (75.73% Cu, 4.28% Si) which was quenched in water at 600°C. after being heated for 120 hours. The large twinned crystals are δ and the small light crystals are silicon. The latter are always observed to be greyish-blue under the microscope.

We see in the alloy TSA 423 (72.91% Cu, 4.0% Si) that the ε_{2a} phase separates primarily, and this alloy solidifies with the reaction liquid $\rightarrow \varepsilon_{2a} + \mathrm{Si}$. The $\varepsilon_{2a} + \mathrm{Si}$ phase is transformed into $\zeta_1 + \delta + \mathrm{Si}$ at 560°C. and finally into $\zeta_2 + \delta + \mathrm{Si}$ at 530°C. Hence such an alloy consists of $\zeta_2 + \delta + \mathrm{Si}$ at below 530°C, as shown in photograph 17.

The alloy TSA 426 (Cu 70%, Si 4%) consists of $\varepsilon_{2a} + \eta_1 + \mathrm{Si}$, when it has just solidified but it is changed into $\zeta_1 + \eta_1 + \mathrm{Si}$, $\zeta_2 + \eta_1 + \mathrm{Si}$, and finally $\zeta_2 + \eta_2 + \mathrm{Si}$, hence it consists of $\zeta_2 + \eta_2 + \mathrm{Si}$ below 560°C. This is illustrated in photograph 18, in which the dendritic η_2 crystals are surrounded by the mixture of $\zeta_2 + \mathrm{Si}$.

Photograph 19 shows the microstructure of the furnace-cooled alloy TSA 430 (Cu 66.0)%, Si 4.21%), in which decomposed η_2 crystals are present with the white θ and greyish-blue silicon crystals.

2) The microstructures of alloys containing 1 per cent. of aluminium and 0-17 per cent. of silicon.

The results of the microscopical examinations are shown in Table 28.

Photograph 20 shows the structure of an alloy containing 6.63 per cent. of silicon and 92.37 per cent. of copper, which was heated at 800°C. and cooled to 760°C in the furnace and annealed for 30 minutes at that temperature and then quenched in water. It is included to illustrate the

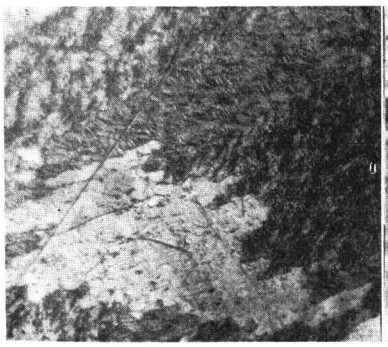

(13) TSA 125 (73.88% Cu, 1.19% Si)
Quenched at 550°C.
ζ_1+Si. ×150.

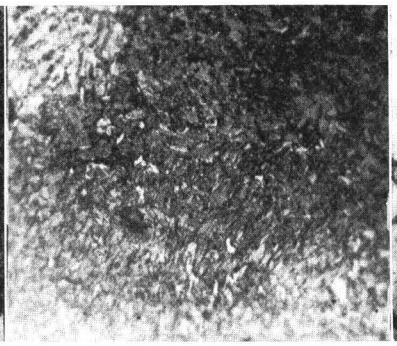

(14) TSA 227 (71.00% Cu, 2.00% Si)
Quenched at 500°C.
$\zeta_2+\eta_2$+Si. ×150.

(15) TSA 128 (70.73% Cu, 1.26% Si)
Quenched at 570°C.
η_1+Si. ×150

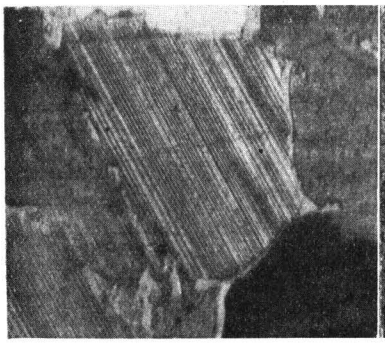

(16) TSA 420 (75.73% Cu, 4.28% Si)
Quenched at 600°C.
twinned δ+Si. ×100

(17) TSA 423 (72.91% Cu, 4.00% Si)
Furnace cooled.
$\zeta_2+\delta$+Si. ×100.

(18) TSA 426 (70% Cu, 4% Si)
Furnace cooled.
$\eta_2+\zeta_2$+Si. ×100.

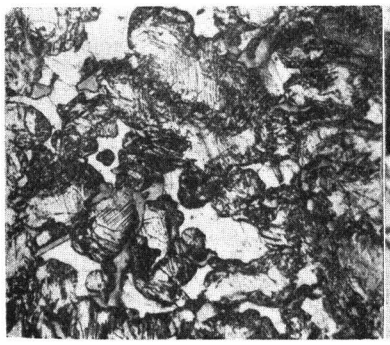

(19) TSA 430 (66.09% Cu, 4.21% Si)
Furnace cooled.
$\eta_2+\theta$+Si. ×100.

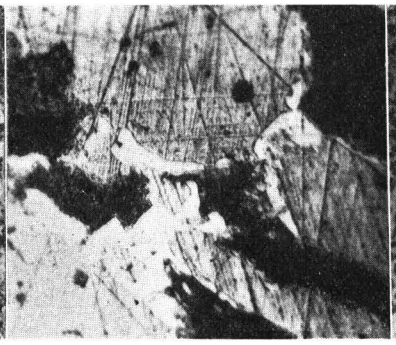

(20) T 17 (6.63% Si, 92.34% Cu)
Quenched at 765°C.
$\alpha+\beta+\gamma_t$. ×100.

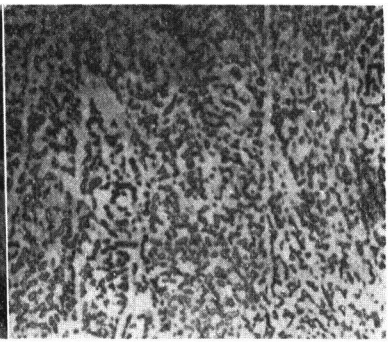

(21) T 17.5 (7.21% Si, 91.55% Cu)
Quenched at 600°C.
$\alpha+\gamma_s$. ×100.

(22) T 18 (7.98% Si, 90.77% Cu)
Annealed for 1 month at
450°C. and quenched in water.
γ_s. ×100.

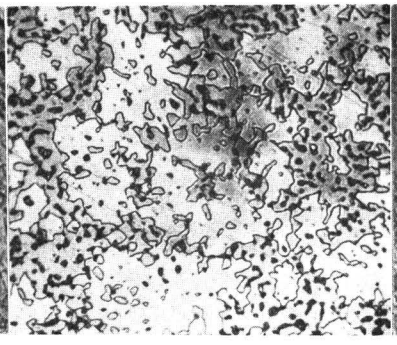

(23) T 19 (8.78% Si, 90 11% Cu)
Quenched at 600°C.
$\gamma_s+X+\alpha$. ×100.

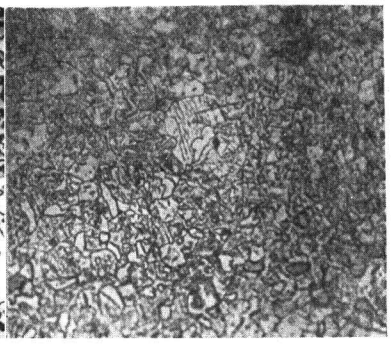

(24) T 110 (9.72% Si, 89.26% Cu)
Quenched at 760°C.
$\gamma_t+\varepsilon_s$. ×100.

Table 28.

No.	Quenching Temp. °C	Heating Time. (hours)	Phases.
T 14	850	6	α
,,	600	120	α
,, 15	830	4	α
,,	600	120	α
TSA 601	830	4	$\alpha+\beta$
,,	600	120	$\alpha+\gamma_s$
T 17	800	6	$\beta+\alpha$
,,	770	4	$\alpha+\beta$
,,	765	0 5	$\alpha+\beta+\gamma_t$
,,	760	1	$\alpha+\gamma_t$
,,	690	18	$\alpha+\gamma_t$
,,	600	120	$\alpha+\gamma_s$
,, 17.5	800	6	β (decomposed)
,,	700	4	β (decomposed)
,,	600	120	$\alpha+\gamma_s$
,, 18	800	6	β (decomposed)
,,	770	4	$\beta+\gamma_t$
,,	750	12	$\alpha+\gamma_t$
,,	600	120	almost γ_s
,,	450	1 month	γ_s
,, 18.5	800	6	$\beta+\gamma_t$
,,	750	12	$\gamma_t+\alpha$
,,	600	120	γ_s+X
,, 19	800	6	γ_t
,,	760	8	γ_t
,,	600	120	$\gamma_s+X+\alpha$
,,	450	1 month	$\gamma_s+X+\alpha$
,, 19.5	760	8	γ_t+a little ε_s
,,	740	18	γ_t+X
,,	600	120	$\gamma_s+X+\alpha$
,,	450	1 month	$X+\alpha$
,, 110	760	8	$\gamma_t+\varepsilon_s$
,,	740	18	γ_t+X
,,	700	14	γ_t+X
,,	600	120	$X+\alpha$
,,	450	1 month	$X+\alpha+\varepsilon_s''$
,, 110 5	760	8	$\gamma_t+\varepsilon_s$
,,	700	14	$X+\gamma_t$
,,	600	120	$X+\alpha$
,, 111	760	8	$\gamma_t+\varepsilon_s$
,,	700	14	$X+\varepsilon_s$
,,	600	120	$X+\varepsilon_s'$
,,	450	1 month	$X+\varepsilon_s''+\alpha$
,, 111.5	760	8	$\gamma_t+\varepsilon_s$
,,	700	14	ε_s+X
,,	600	120	ε_s+X
TSA 1201	760	8	ε_s
,,	700	14	ε_s
,,	600	120	ε_s'+a very little X
,,	450	1 month	ε_s''+a very little X
T 112.5	760	8	ε_s
,,	600	120	ε_s
,,	450	1 month	ε_s''+Si
,, 113.5	700	14	ε_s+Si
,,	600	120	ε_s+Si
,,	550	28	ε_s'+Si
,,	450	1 month	ε_s''+Si
,, 115	600	120	ε_s+Si
,,	550	28	ε_s'+Si
,,	450	1 month	ε_s''+Si

three-phase field of $\alpha+\beta+\gamma_t$. In this figure we see that the black portion is the decomposed β phase, and the small light, grey, crystal is the γ_t phase. The structure of the two-phase field of $\gamma_s+\alpha$ is similar to that in the binary Cu-Si system. It is shown in photograph 21, in which the grey etching constituents are the γ_s phase in the matrix of α phase. The γ_s phase forms a range of solid solution, the maximum solubility of which with aluminium may be less than 1.5 per cent. at about 450°C. Photograph 22 is the photo-micrograph of T 18 (Si 7.98%, Cu 99.77%), in which the homogeneity exhibited by γ_s is seen. The alloy containing 8.78 per cent. of silicon and 90.11 per cent. of copper consists of the γ_t phase, when it has just solidified, but it is changed into, $\gamma_t+\gamma_s$, $\gamma_t+\gamma_s+X$, and γ_s+X on cooling, and lastly it is transformed into $\gamma_s+X+\alpha$. Photograph 23 shows such a structure of the $\gamma_s+X+\alpha$ etched deeply with ferric chloride solution, in which the dark etching constituents α and the grey X crystals are in the matrix of the γ_s phase.

T 110 is an alloy containing 9.72 per cent. of silicon and 89.26 per cent. of copper. It commences to solidify with the primary crystallization of γ_t and completes it with the reaction, Liquid $\rightarrow\gamma_t+\varepsilon_s$. Photograph 26 shows such a structure in which decomposed γ_t crystals are surrounded with the light reddish ε_s crystals.

The temperature of the binary peritectoid reaction, $\gamma_t+\varepsilon_s \rightleftarrows X$, falls with the addition of aluminium as previously illustrated in the results of the thermal analysis. It is also evident in the microscopic examination that the T 110 alloy consists of $\gamma_t+\varepsilon_s$ at the temperature 760°C. We see such a structure in Photograph 24, in which the ε_s crystals are existent in the boundary of the γ_t crystals. In the same alloy, heated for 18 hours at 740°C. and quenched, we see that it consists of γ_t+X only. This is shown in photograph 25, under a magnification of 100 diameters. If the same alloy is slowly cooled from 740°C. to 600°C., the change of the microstructure is marked. At this temperature, we see that in the three-phase field of $X+\gamma_s$+a little α is present.

The ε_s phase extends from about 11.7 to 12.8 and from 12 to 12.6 per cent. of silicon at 700° and 450°C. respectively.

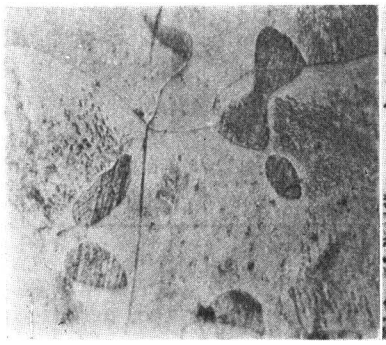

(**25**) T 110 (9.72% Si, 89.27% Cu)
Quenched at 740°C.
γ_t+X. × 100.

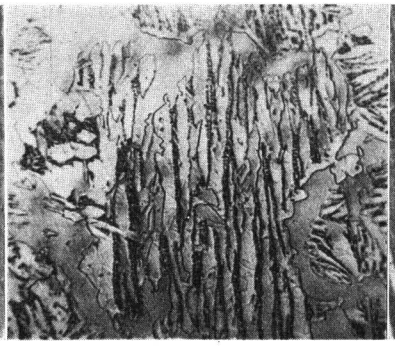

(**26**) T 110 (9.72% Si, 89.26% Cu)
Furnace cooled.
Decomposed $\gamma_t+\varepsilon_s$. × 100.

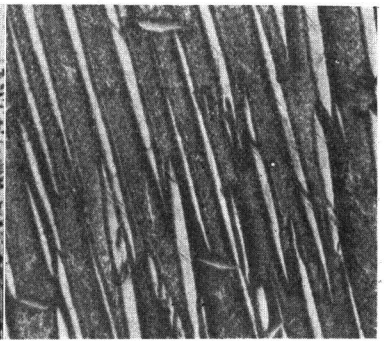

(**27**) T 28.5 (8.42% Si, 89.39% Cu)
Furnace cooled.
Decomposed γ_t. × 50.

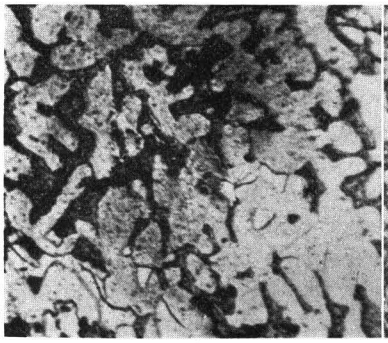

(**28**) T 28.5 (8.42% Si, 89.39% Cu)
Quenched at 600°C.
γ_t+X+α. × 300.

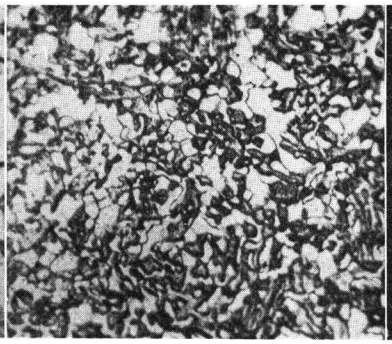

(**29**) T 38 (89.62% Cu, 7.47% Si)
Quenched at 600°C.
γ_t+X+α. × 100.

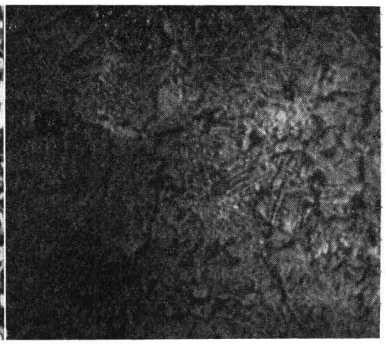

(**30**) T 38 (89.62% Cu, 7.47% Si)
Quenched at 450°C.
$\gamma_t+\varepsilon_s''+\alpha$. × 100.

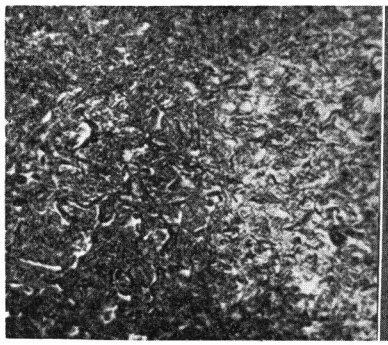

(**31**) T 47 (89.35% Cu, 6.54% Si)
Quenched at 450°C.
$\gamma_t+\varepsilon_s''+\alpha$. × 100.

(**32**) T 48 (88.30% Cu, 7.63% Si)
Quenched at 600°C.
X+γ_t. × 100.

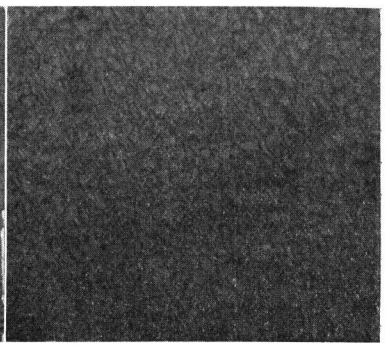

(**33**) T 608 (86.0% Cu, 6.0% Si)
Quenched at 600°C.
$\gamma_t+\varepsilon_s$. × 100.

(**34**) TSA 1006 (83.88% Cu, 10.62% Si)
Quenched at 600°C.
$\gamma_t+\varepsilon_s$+Si. × 100.

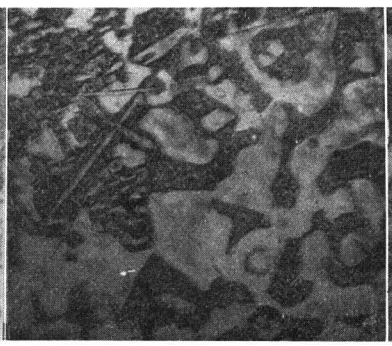

(**35**) TSA 1005 (85.0% Cu, 10.11% Si)
Furnace cooled.
$\gamma_t+\varepsilon_s''$+Si. × 100.

(**36**) TSA 1208 (80.0% Cu, 12% Si)
Furnace cooled.
Si+$\gamma_t+\varepsilon_s''$. × 150.

3) The microstructures of alloys containing 2–6 per cent. of aluminium and 0–15 per cent. of silicon.

From the microstructures of alloys containing 2, 3, 4 and 6 per cent. of aluminium and 0–15 per cent. of silicon the present writer has ascertained the existence of the two invariant reactions in solid state, $\gamma_\ell+\gamma_s \rightleftarrows X+\alpha$, $\gamma_\ell+X \rightleftarrows \varepsilon_s''+\alpha$, as they have been already confirmed by the thermal analysis. The changes of microstructures of these alloys are summarized in Table 29.

Table 29.

No.	Quenching Temp. °C	Heating Time. (hours)	Phases.
	T 2 Series.		
TSA 602	800	4	$\alpha+\beta$
,,	740	18	$\alpha+\gamma_\ell$
T 27	770	6	β
,,	700	14	$\alpha+\gamma_\ell$
,,	600	120	$\alpha+X$
,, 27.5	770	6	β
,,	700	14	$\alpha+\gamma_\ell$
,,	450	1 month	$\alpha+X$
,, 28	800	4	γ_ℓ+a little β
,,	770	6	$\gamma_\ell+\beta$
,,	600	120	$\gamma_\ell+X+\alpha$
,, 28.5	800	4	γ_ℓ
,,	770	6	γ_ℓ
,,	600	120	$\gamma_\ell+X+\alpha$
,, 29	800	4	γ_ℓ
,,	770	6	γ_ℓ
,,	700	2	$\gamma_\ell+X$
,,	600	120	$\gamma_\ell+X+\alpha$
,,	450	1 month	$X+\varepsilon_s''+\alpha$
,, 29.5	770	6	$\gamma_\ell+\varepsilon_s$
,,	700	2	$\gamma_\ell+X$
,,	600	120	$\gamma_\ell+X+\alpha$
,,	450	1 month	$X+\varepsilon_s''+\alpha$
TSA 1002	740	18	$\gamma_\ell+\varepsilon_s$
,,	600	120	$X+\gamma_\ell+\varepsilon_s$
,,	450	1 month	$X+\varepsilon_s''+\alpha$
T 211	740	18	ε_s+X
,,	600	120	$X+\varepsilon_s+\gamma_\ell$
,,	450	1 month	$X+\varepsilon_s''+\alpha$
TSA 1202	740	18	ε_s
,,	600	120	ε_s+a very little X
T 213	740	18	ε_s+Si
,,	600	120	ε_s+Si
,, 215	600	120	$\varepsilon_s+\gamma_\ell$+Si
,,	450	1 month	$\varepsilon_s''+\gamma_\ell$+Si
	T 3 Series.		
TSA 603	800	12	α+a very litt e β
,,	600	120	$\alpha+\gamma_\ell$
T 37	800	12	β
,,	780	4	β
,,	770	2	β+a little γ_ℓ
,,	600	120	$\alpha+\gamma_\ell$
,,	450	1 month	$\alpha+\gamma_\ell+\varepsilon_s''$
,, 38	800	12	$\beta+\gamma_\ell$
,,	760	4	$\beta+\gamma_\ell$
,,	700	2	$\gamma_\ell+\alpha$
,,	600	120	$\gamma_\ell+\alpha+X$
,,	450	1 month	$\gamma_\ell+\varepsilon_s''+\alpha$
,, 39	800	12	γ_ℓ
,,	760	4	γ_ℓ
,,	600	120	$\gamma_\ell+X$
,,	450	1 month	$\gamma_\ell+\varepsilon_s''+\alpha$
,, 310	760	4	$X+\gamma_\ell$
,,	600	120	$X+\gamma_\ell+\varepsilon_s$
,,	450	1 month	$\gamma_\ell+\varepsilon_s''+\alpha$
,, 311	740	2	$\varepsilon_s+\gamma_\ell$
,,	600	120	ε_s+X
,,	450	1 month	$\varepsilon_s''+\gamma_\ell+\alpha$
,, 312	700	2	$\varepsilon_s+\gamma_\ell$
,,	600	120	$\varepsilon_s+\gamma_\ell$+Si
,,	450	1 month	$\varepsilon_s''+\gamma_\ell$+Si
,, 314	700	2	$\varepsilon_s+\gamma_\ell$+Si
,,	600	120	$\varepsilon_s+\gamma_\ell$+Si
,,	450	1 month	$\varepsilon_s''+\gamma_\ell$+Si
	T 4 Series.		
TSA 604	800	12	β+a little α
,,	700	2	$\beta+\alpha$
,,	600	120	$\alpha+\gamma_\ell$
,,	450	1 month	$\alpha+\gamma_\ell+\varepsilon_s''$
T 47	800	12	β
,,	760	4	$\beta+\gamma_\ell$
,,	600	120	$\gamma_\ell+\alpha$
,,	550	8	$\alpha+\gamma_\ell+X$
,,	450	1 month	$\alpha+\gamma_\ell+\varepsilon_s''$
,, 48	760	4	γ_ℓ
,,	650	18	γ_ℓ
,,	600	120	$\gamma_\ell+X$
,,	570	4	$\gamma_\ell+X$
,,	550	8	$\gamma_\ell+X+\alpha$
,,	450	1 month	$\gamma_\ell+\varepsilon_s''+\alpha$
,, 49	700	2	$\gamma_\ell+\varepsilon_s$
,,	650	18	$\gamma_\ell+X+\varepsilon_s$
,,	550	8	$\gamma_\ell+X$
,,	450	1 month	$\gamma_\ell+\varepsilon_s''+\alpha$
,, 410	650	18	$\varepsilon_s+\gamma_\ell$
,,	600	120	$\varepsilon_s+\gamma_\ell$
,,	450	1 month	$\varepsilon_s''+\gamma_\ell+\alpha$
,, 411	600	120	$\varepsilon_s+\gamma_\ell$+Si
,,	450	1 month	$\varepsilon_s''+\gamma_\ell$+Si
TSA 1204	600	120	$\varepsilon_s+\gamma_\ell$+Si
,,	450	1 month	$\varepsilon_s''+\gamma_\ell$+Si
T 414	600	120	$\varepsilon_s+\gamma_\ell$+Si
,,	450	1 month	$\varepsilon_s''+\gamma_\ell$+Si
	T 6 Series.		
T 605	700	2	β

„	600	120	$\alpha+\gamma_t$
„ 606	800	6	β
„	700	2	$\beta+\gamma_t$
„	600	120	$\alpha+\gamma_t$
„	450	1 month	finely decomposed $\gamma_t+\alpha$
„ 607	800	6	$\beta+\gamma_t$
„	700	2	$\beta+\gamma_t$
„	600	120	$\gamma_t+\alpha$
„	450	1 month	$\gamma_t+X+\alpha$
„ 608	700	2	$\gamma_t+\varepsilon_s$
„	600	120	$\gamma_t+\varepsilon_s$
„	450	1 month	decomposed $\gamma_t+\alpha$
„ 609	700	2	$\gamma_t+\varepsilon_s+Si$
„	600	120	$\gamma_t+\varepsilon_s+Si$
„	550	8	$\gamma_t+\varepsilon_s'+Si$
„	450	1 month	$\gamma_t+\varepsilon_s''+Si$
TSA 1006	600	120	$\gamma_t+\varepsilon_s+Si$
„	450	1 month	$\gamma_t+\varepsilon_s''+Si$
T 611	600	120	$\gamma_t+\varepsilon_s+Si$
„	450	1 month	$\gamma_t+\varepsilon_s''+Si$
„ 614	600	120	$\gamma_t+\varepsilon_s+Si$
„	450	1 month	$\gamma_t+\varepsilon_s''+Si$

The alloy T 28.5 (8.42% Si, 89.39% Cu) solidifies in the γ_t crystals, which are transformed into a complex structure with the peritectoid reaction, $\gamma_t+\gamma_s\rightarrow X+\alpha$. This is illustrated in the micrograph of the furnace cooled specimen (Photograph 27). When the alloy is annealed and quenched above about 700°C., the decomposed γ_t phase is seen to be the same as the structure of the binary Cu-Si alloy. But if this T 28.5 alloy is heated at temperatures between 670°–550°C. and quenched in water, the three-phase field of $\gamma_t+X+\alpha$ due to the above described invariant reaction, is distinctly observed, as shown under a magnification of 300 diameters in photograph 28.

The similar structure of the $\gamma_t+X+\alpha$ phases is also seen in alloys containing 3–4 per cent. of aluminium shown in photograph 29. Photograph 29 is the microstructure of T 38 (Cu 89.62%, Si 7.47%) alloy, in which the grey etching constituents are the γ_t phase and the dark grey coloured X phase is seen in the boundary of the γ_t phase. α is coloured yellowish grey when it is etched with ferric chloride solution. In the same alloy heated for one month at 450°C. and quenched, however, we see that the $\gamma_t+X+\alpha$ phase is transformed into the $\gamma_t+\varepsilon_s''+\alpha$ phase by the peritectoeutectoid reaction $\gamma_t+X\rightleftarrows\varepsilon_s''+\alpha$. Photograph 30 illustrates such a structure, in which the black portion is the α phase and complex structures $\gamma_t+\varepsilon_s''$ is distinctly observed. A similar phenomenon is also seen in the alloy T 47 (Cu 89.35%, Si 6.54%), which is annealed at 450°C and quenched at that temperature. It is shown in photograph 31.

The alloy T 48 (Cu 88.3%, Si 7.63%) consists also only of the γ_t phase, when it has just solidified, but this γ_t phase is changed into γ_t+X on cooling from about 630°C. Photograph 32 illustrates such a structure, in which small needle X crystals are distributed in the matrix of the γ_t phase.

T 608 is an alloy containing 86.0 per cent. of copper and 6.0 per cent. of silicon. It commences to solidify with the primary crystallization of γ_t and completes it with the reaction Liquid $\rightarrow\gamma_t+\varepsilon_s$. Hence such an alloy consists of the two-phase field of the temperature below the solidus, as in photograph 33. In the figure we see that white crystals γ_t are present with the grey ε_s crystals.

Photograph 34 represents a structure of an alloy containing 83.88 per cent. of copper and 10.62 per cent. of silicon. It is typical of the three-phase field of $\gamma_t+\varepsilon_s+Si$.

4) The microstructures of alloys containing 6, 10, 12 and 20 per cent. of silicon and varying content of aluminium.

Specimens in the above described four constitutional sections were also annealed at various temperatures for a long time, and quenched at that temperature.

Although we see no peculiar structures to speak of, here we will briefly comment on the results of the microscopical examination, shown in the following table.

Table 30.

No.	Quenching Temp. °C	Heating Time. (hours)	Phases.
TSA 6 Series.			
TSA 605	800	12	β
„	700	2	$\beta+\gamma_t$
„	600	120	$\gamma_t+\alpha$
„	450	1 month	$\gamma_t+\varepsilon_s''+\alpha$
„ 607	800	12	$\beta+\gamma_t$
„	700	2	$\beta+\gamma_t$
„	600	120	$\gamma_t+\alpha$
„	450	1 month	$\gamma_t+\varepsilon_s''+\alpha$
„ 608	700	2	γ_t
„	600	120	γ_t
„	500	8	γ_t
„ 609	700	2	γ_t
„	600	120	γ_t+a little ε_s
„	450	1 month	$\gamma_t+\varepsilon_s''$
„ 610	700	2	γ_t+Si
„	600	120	γ_t+Si
„ 613	700	2	γ_t+Si
„	600	120	γ_t+Si
„	450	1 month	γ_t+Si

,, 618	700	2	γ_t+Si
,, 620	700	2	$\gamma_t+\varepsilon_{2a}$+Si
,,	600	120	$\gamma_t+\delta$+Si
,,	450	1 month	$\gamma_t+\delta$+Si
,, 623	600	120	ε_{2a}+Si
,,	450	1 month	$\delta+\zeta_2$+Si
,, 629	600	120	η_1+Melt
,,	450	1 month	η_2+Si
,, 630	450	1 month	$\eta_2+\theta$+Si
TSA 10 Series.			
TSA 1005	700	2	$\gamma_t+\varepsilon_s$+Si
,,	600	120	$\gamma_t+\varepsilon_s$+Si
,,	450	1 month	$\gamma_t+\varepsilon_s''$+Si
,, 1008	700	2	$\gamma_t+\varepsilon_s$+Si
,,	600	120	$\gamma_t+\varepsilon_s$+Si
,,	450	1 month	$\gamma_t+\varepsilon_s''$+Si
,, 1009	700	2	γ_t+Si
,,	600	120	γ_t+Si
,,	450	1 month	$\gamma_t+\varepsilon_s''$+Si
,, 1012	700	2	γ_t+Si
,,	600	120	γ_t+Si
,,	450	1 month	γ_t+Si
,, 1015	700	2	γ_t+Si
,,	600	120	γ_t+Si
,, 1020	700	2	$\gamma_t+\varepsilon_{2a}$+Si
,,	600	120	$\delta+\varepsilon_{2a}$+Si
,, 1025	600	120	$\varepsilon_{2a}+\eta_1$+Si
,,	450	1 month	$\zeta_2+\eta_2$+Si
TSA 12 Series.			
TSA 1205	700	2	$\gamma_t+\varepsilon_s$+Si
,,	600	120	$\gamma_t+\varepsilon_s$+Si
,, 1208	600	120	$\gamma_t+\varepsilon_s$+Si
,, 1210	600	120	γ_t+Si
,, 1215	600	120	γ_t+Si
,, 1220	600	120	$\varepsilon_{2a}+\delta$+Si
,,	500	120	$\delta+\zeta_2$+Si
,, 1225	600	120	η_1+Si
,,	500	120	η_2+Si
,, 1230	500	120	$\eta_2+\theta$+Si
TSA 20 Series.			
TSA 2005	700	2	$\gamma_t+\varepsilon_s$+Si
,,	600	120	$\gamma_t+\varepsilon_s$+Si
,,	500	120	$\gamma_t+\varepsilon_s''$+Si
,, 2010	600	120	γ_t+Si
,,	500	120	γ_t+Si
,, 2015	600	120	γ_t+Si
,,	500	120	γ_t+Si
,, 2020	600	120	ε_{2a}+Si
,,	500	120	$\delta+\zeta_2$+Si
,, 2025	500	120	$\eta_2+\theta$+Si
,, 2030	500	120	$\eta_2+\theta$+Si
,, 2040	500	120	$\theta+\chi$+Si
,, 2050	500	120	$\theta+\chi$+Si
,, 2060	500	120	$\chi+\theta$+Si

These results of microscopical study being taken into consideration the sectional diagrams as shown in Figures 17–20 are obtained.

Photograph 35 represents the microstructure of the furnace cooled alloy TSA 1005 containing Cu 85.0 per cent. and Si 10.11 per cent. In the figure the primary separation γ_t appears in dendritic form, surrounded by the binary eutectic $\gamma_t+\varepsilon_s$ and the ternary eutectic $\gamma_t+\varepsilon_s+$Si.

In the alloy TSA 1208 (Cu 80.0%, Si 12%) the Si crystals separate primarily in angular form, and the binary eutectic reaction Liquid$\rightarrow\gamma_t+$Si takes place subsequently. Finally it solidifies with the ternary eutectic reaction Liquid$\rightarrow\gamma_t+\varepsilon_s+$Si. This is illustrated in the micrograph of the furnace-cooled alloy (Photograph 36). Photograph 37, under a magnification of 100 diameters, shows the structure of an alloy containing 12 per cent. of silicon and 68 per cent. of copper which has been very slowly cooled from the molten state. Small needles of silicon appear in the crystals of $\zeta+\delta$. This structure supports the existence of the reaction $\varepsilon_{2a}\rightarrow\delta+\zeta+$Si.

C. The Copper Solid Solution.

The present writer, during work connected with another aspect of the copper-silicon-aluminium system, has determined the solubility of silicon and aluminium in solid copper in a separate series of alloys, since a knowledge of the position of the α-phase boundary is of importance in practice.

Annealing of the specimens was carried out for 8 hours at 800°C, for a day or more, at the lower temperatures above 600°C and for one month at 400°C. To obtain complete equilibrium conditions the samples were first quenched from a high temperature at which they were homogeneous, and then re-annealed at the desired temperatures.

The structures observed in the various quenched samples are given in Table 31. Figures 30–33 indicate the horizontal sections (isotherms) at 800°, 700°, 600°, and 400°C., respectively, which have been described, corresponding to those of the vertical sections in Figures 15–26, thus ensuring a greater accuracy than would be obtained by simple plotting in one plane or set of planes. The α-phase boundary in this ternary system at constant temperature is concave to the copper corner.

The solubility of silicon in α-phase near the Cu-Si side reaches a maximum at about 700°C. and decreases above and below this temperature. At a temperature of 700°C. copper is capable of holding in solid solution about 5.7 per cent. of silicon by the presence of 2 per cent. of aluminium, while at 800° and 600°C. the solubility is about 5.2 and 5.5 per cent. of silicon respectively.

The solubility of aluminium in solid copper is decreased by the presence of silicon; about 1 per

Table 31.

No.	Composition (by analysis)			Heat treatment.			
	Cu%	Si%	Al%	800°–8 hrs.	700°–1 day.	600°–7 day.	400°–1 month.
C 12	97.40	0.85	Rest	α	α	α	α
,, 13	96.03	0.71	,,	α	α	α	α
,, 14	94.71	0.83	,,	α	α	α	α
,, 15	93.95	0.98	,,	α	α	α	α
,, 16	93.43	0.91	,,	α	α	α	α
,, 17	92.05	0.87	,,	α	α	α	α
,, 18	91.10	0.93	,,	α+β	α	α	α
,, 110	89.06	0.97	,,	β	α+β	α+β	α+γ_t
,, 21	97.13	1.89	,,	α	α	α	α
,, 22	96.13	1.91	,,	α	α	α	α
,, 23	95.03	1.97	,,	α	α	α	α
,, 24	93.95	1.98	,,	α	α	α	α
,, 25	92.82	2.11	,,	α	α	α	α
TSA 26	92.11	2.05	,,	α	α	α	α
,, 28	90	2	,,	β+α	β+α	α+β	α+γ_t
,, 210	87.71	2.01	,,	β	β	β+γ_t	α+γ_t
C 32	94.96	2.97	,,	α	α	α	α
,, 34	92.94	2.89	,,	α	α	α	α
,, 36	91.02	2 93	,,	α+β	α	α	α
,, 38	87.97	3.12	,,	β	β	α+γ_t	α+γ_t
,, 41	95.08	3.92	,,	α	α	α	α
,, 42	94.01	3.91	,,	α	α	α	α
,, 43	2.15	3.90	,,	α	α	α	α
,, 45	91.10	4.12	,,	β+α	α	α+γ_t	α+γ_t
,, 46	89.97	4.03	,,	β+α	α+β	α+γ_t	α+γ_t
,, 51	94.20	5.11	,,	α	α	α	α+γ_t
,, 52	93.15	5.17	,,	α	α	α	α+γ_t
,, 54	90.96	5.00	,,	β+α	α+β	α+γ_t	α+γ_t+ε_s''
,, 56	89.04	4.87	,,	β	β	α+γ_t	α+γ_t
T 61	93.15	5.59	,,	α	α	α	α+γ_s
,, 62	92.28	5 79	,,	α+β	α+γ_t	α+γ_s	α+γ_s
,, 63	91.33	5.49	,,	α+β	α+γ_t	α+X	α+γ_t+ε_s''
,, 64	90.16	5.62	,,	β	β+α	α+γ_t	α+γ_t+ε_s''
,, 65	89.18	5.76	,,	β	β+γ_t	α+γ_t	α+γ_t+ε_s''
,, 17	92.34	6.63	,,	α+β	α+γ_t	α+γ_s	α+γ_s
,, 27	90.95	6.87	,,	β	α+γ_t	α+X	α+γ_t+ε_s''
,, 37	90.43	6.52	,,	β	α+γ_t	α+γ_t+X	α+γ_t+ε_s''
,, 47	89.35	6.54	,,	β+γ_t	β+γ_t	α+γ_t	α+γ_t+ε_s''

cent. of silicon reduces the solubility from about 10 per cent. to 9 per cent. of aluminum at 400°C. Greater percentages of silicon have further effect on the solubility of the aluminium in solid copper.

As shown in Figure 30, the isothermal constitutional diagram at 800°C consists of one phase or two phase fields of α, β, γ_t, and ε_s in solid state. Figures 31 and 32, however, show the isothermal constitutional diagrams at 600° and 700°C. in which γ_t, X, and silicon appear in addition to these four phases. Figure 33 indicates that three-phases α_t, γ and ε_s'' coexist in some range at 400°C.

Photographs 38 and 39 show the structures of the two-phase field at 700°C near the α-phase

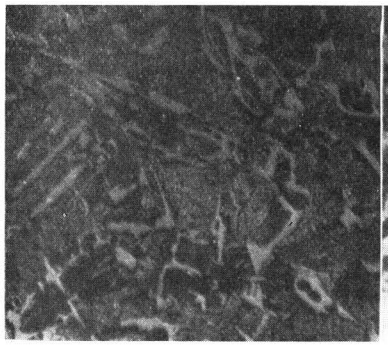

(**37**) TSA 1220 (68% Cu, 12% Si)
Furnace cooled.
$\zeta_2+\varepsilon+$Si. × 00.

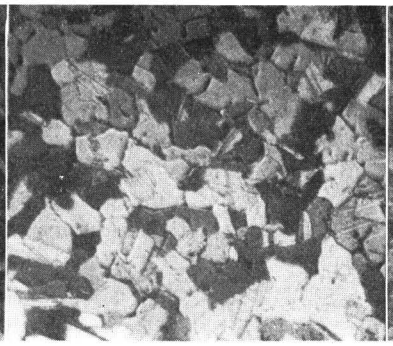

(**38**) C 54 (90.96% Cu, 5.0% Si)
Quenched at 700°C.
α+β. ×150.

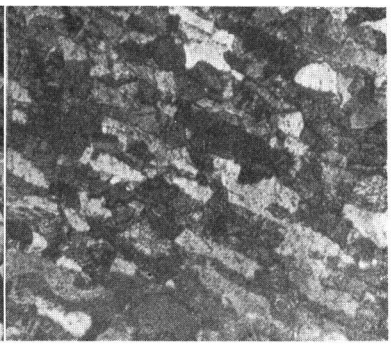

(**39**) T 63 (91.33% Cu, 5 49% Si)
Quenched at 700°C.
α+γ_t. ×100.

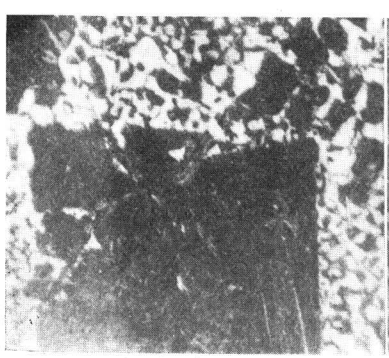

(**40**) CA 7 (44.80% Cu, 2.16% Si)
Furnace cooled.
θ+Si+χ. ×50.

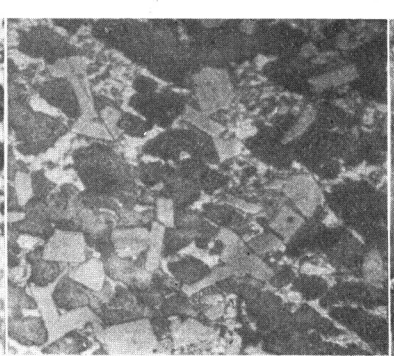

(**41**) CC 5 (35.08% Cu, 5.88% Si)
Furnace cooled.
Si+θ+χ. ×150.

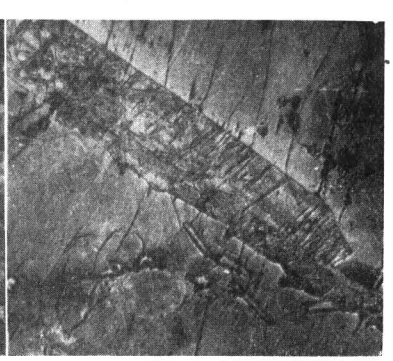

(**42**) TSA 445 (51.18% Cu, 4.03% Si)
Furnace cooled.
γ_{11}+Si+θ. ×100.

Fig. 30

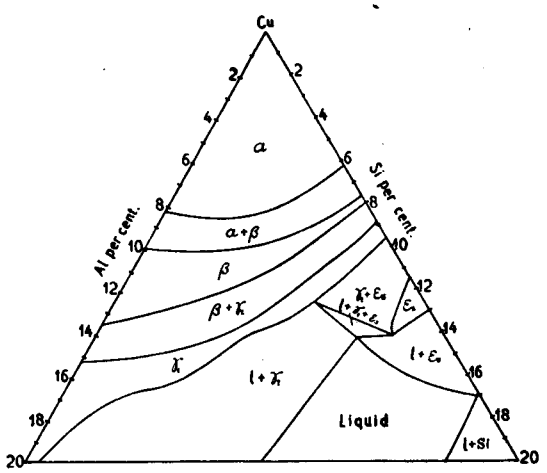

Fig. 31.

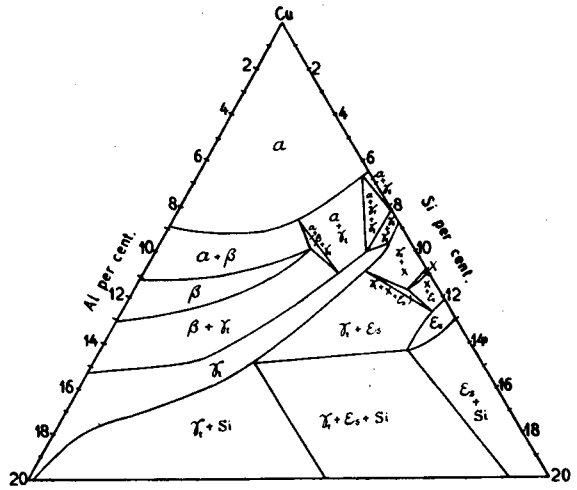

Fig. 32.

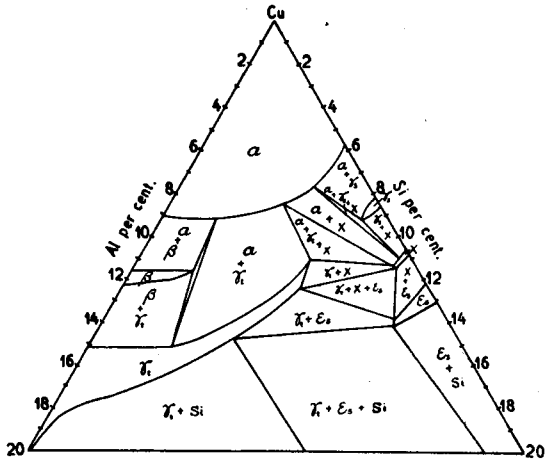

boundary. In the former micrograph we see plainly that small black crystals of β are distributed in the matrix of twinned α, and in the latter we can scarecely see that small greyish crystals of γ_t are present in the boundary of twinned α.

In the α crystals twinning is always observed.

Fig. 33.

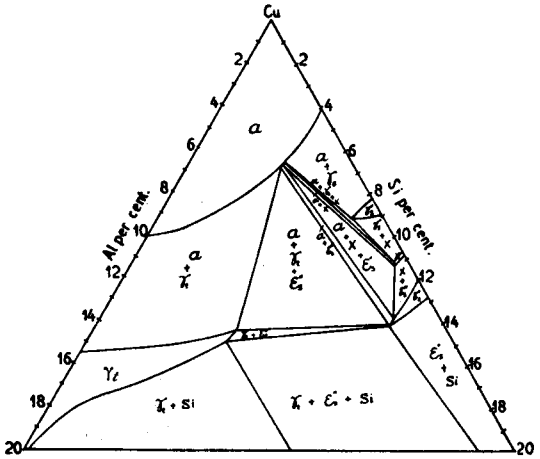

IV. The Constitution of the Al-rich Al-Cu-Si System.

A. Thermal Analysis.

Thermal curves were taken of a series of alloys containing 2, 4, 6 and 8 per cent. of silicon, in which the aluminium content varied in steps of 5–10 per cent. or less, according to necessity. The method employed was identical to that described in the previous paper. The arrest or change points obtained from the cooling curves are shown in Tables 32–35. Figures 34–37 show the sectional diagrams, representing a parallel to the aluminium-copper phase, as derived from both the results of thermal analysis and microscopic examination.

It will be seen from these diagrams that three invariant reactions exist in aluminium corner.

The equilibrium diagram is illustrated in Figure 38, in which the fields of the primary separation

Table 32.

CA Series. (2% Silicon).

No.		Composition. (by analysis)			Points of Change or Arrest. °C.			
		Cu%	Si%	Al%				
CA	1	9.98	1.89	Rest	621		524	520
,,	2	20.01	2.00	,,	590		542	517
,,	3	25.12	2.13	,,	563		548	518
,,	4	30.05	2.09	,,	546			521
,,	5	34.65	2.03	,,	550			522
,,	6	39.70	2.01	,,	566			524
,,	7	44.80	2.16	,,	575		530	521
TSA	248	49.36	2.18	,,	578		520	
,,	247	51.03	2.22	,,	580		572	518
,,	246	51.91	2.31	,,	580		573	
,,	245*	53.00	2.00	,,	590		578	570
,,	244	53.85	2.20	,,	602		573	
,,	240	57.14	2.03	,,	625	608	573	568
,,	235*	63.00	2.00	,,	690	614	574	570

* Not analyzed. Composition given as mixed.

Table 33.

CB Series. (4% Silicon).

No.		Composition. (by analysis) Cu%	Si%	Al%	Points of Change or Arrest. °C.				
CB	1	10.00	4.02	Rest	603	543	520		
,,	2	21.00	3.85	,,	554	528	517		
,,	3	25.62	4.12	,,	538		523		
,,	4	30.02	4.04	,,	537		523		
,,	5	34.92	3.95	,,	550		523		
,,	6	40.31	4.17	,,	560		523		
TSA	450	46.28	3.92	,,	575		520		
,,	445	51.18	4.03	,,	580	570	556		
,,	440*	56.00	4.00	,,	620	606	586	568	
,,	435	61.13	3.89	,,	679	624	610	568	558

* Not analyzed. Composition given as mixed.

Table 34.

CC Series. (6% Silicon).

No.		Composition. (by analysis) Cu%	Si%	Al%	Points of Change or Arrest. °C.					
CC	1	9.85	5.86	Rest	593	560	522			
,,	2	14.03	6.11	,,	575	548	521			
,,	3	20.33	6.02	,,	550		523			
,,	4	27.88	6.24	,,	535		522			
,,	5	35.08	5.88	,,	550	537	522			
,,	6	40.17	5.96	,,	561	550	523			
,,	7	48.23	6.00	,,	575		523			
,,	8	51.06	6.03	,,	592	573				
,,	9	54.00	5.89	,,	626	606	588		570	
,,	10	57.31	6.12	,,	634	608	590		569	
,,	11	60.67	5.93	,,	651	636	600	584	567	558

of $\varkappa$(Al), θ, η_1, ε_{2a}, and silicon are respectively represented by JIO_8P', HO_7O_8I, GO_6O_7H, $FO_4O_5O_6G$, and $SiP'O_8O_7O_6O_5$.

Table 35.

CD Series. (10% Silicon).

No.		Composition. (by analysis) Cu%	Si%	Al%	Pointe of Change or Arrest. °C.			
CD	1	5.03	10.06	Rest	575	565	520	
,,	2	10.14	10.15	,,	563		522	
,,	3	15.08	9.92	,,	570	550	519	
,,	4	20.13	10.00	,,	575	541	522	
,,	5	25.00	9.85	,,	585		523	
,,	6*	30.00	10.00	,,	600	534	521	
,,	7	40.15	9.83	,,	650	563	518	
,,	8*	45.00	10.00	,,	676	568	518	
,,	9	50.30	9.86	,,	700	608	572	568
,,	10	55.27	10.32	,,	760	647	607	572

* Not analyzed. Composition given as mixed.

Table 36.

Reaction curve.	Reaction.
Binary eutectic curve, IO_8	Liquid $\rightleftarrows \varkappa + \theta$
,, ,, ,, $P'O_8$	,, $\rightleftarrows \varkappa + Si$
,, ,, ,, O_7O_8	,, $\rightleftarrows \theta + Si$
,, ,, ,, O_6O_7	,, $\rightleftarrows \eta_1 + Si$
,, ,, ,, O_5O_7	,, $\rightleftarrows \varepsilon_{2a} + Si$
,, peritectic curve, HO_7	,, $+\eta_1 \rightleftarrows \theta$
,, ,, ,, GO_6	,, $+\varepsilon_{2a} \rightleftarrows \eta_1$
,, eutectoid curve, W_1w_1	$\varkappa \rightleftarrows \theta + Si$

The binary complex lines showing the univariant reaction are summarized in Table 36.

As already reported in the investigation of the binary Cu-Al system, the typical enveloping structures, due to both peritectic reactions; Liquid $+\varepsilon_{2a} \rightleftarrows \eta_1$, and Liquid $+\eta_1 \rightleftarrows \theta$, also are not observed in the ternary system under microscopic ex-

Fig. 34. CA Series. (2% Silicon).

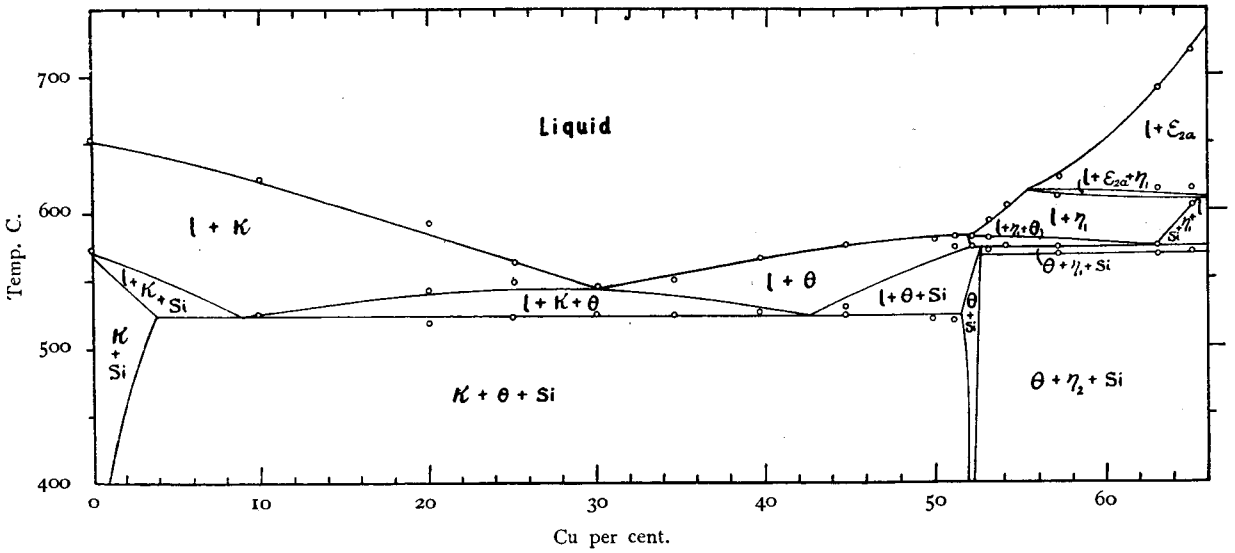

Fig. 35. CB Series. (4% Silicon).

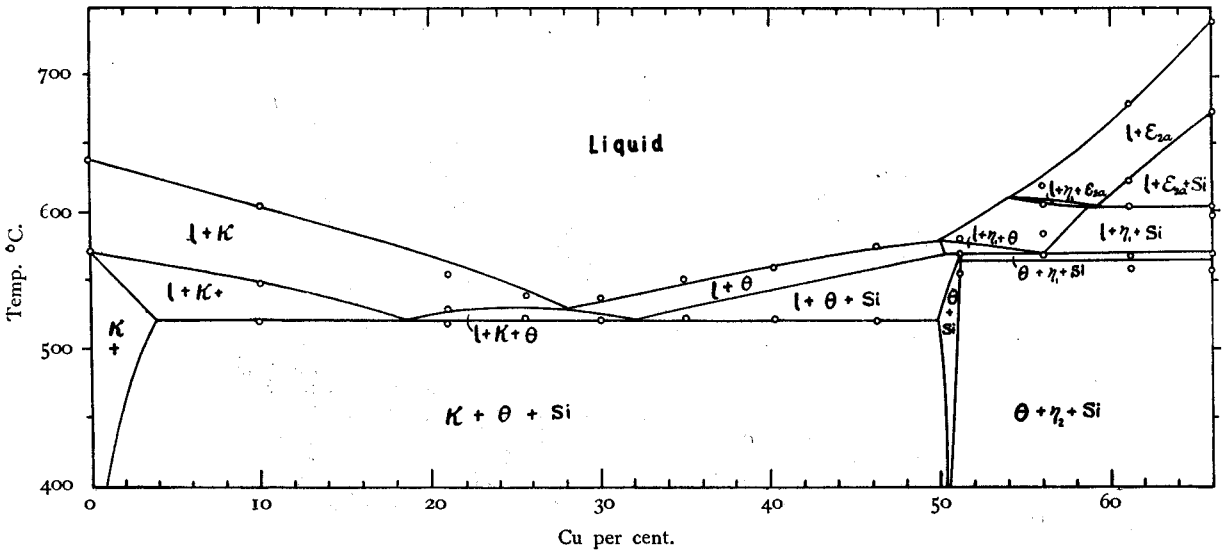

Fig. 36. CC Series. (6% Silicon).

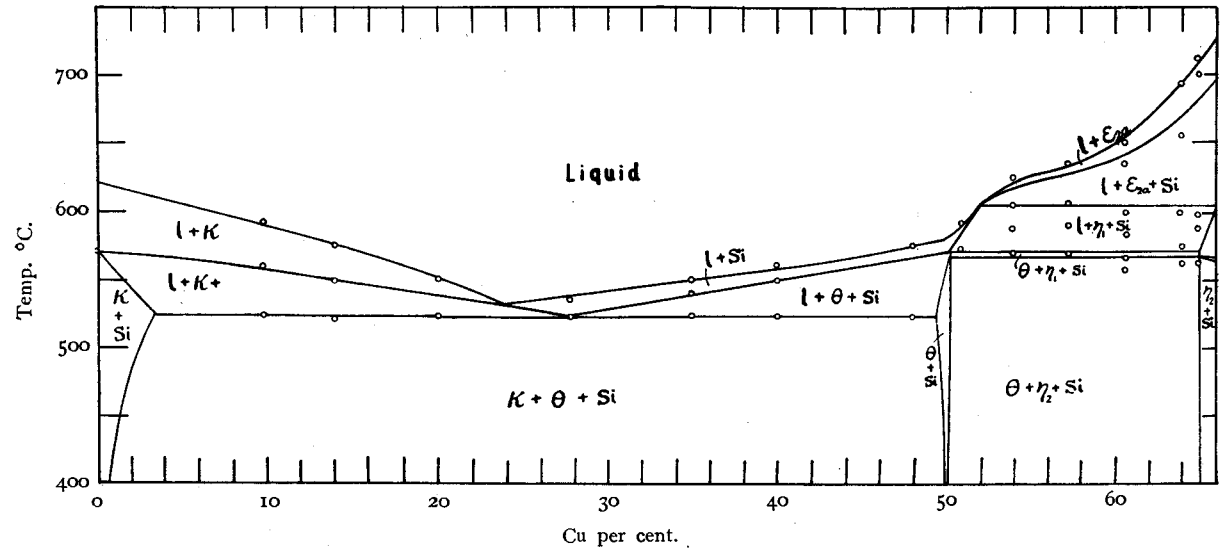

Fig 37. CD Series. (10% Silicon).

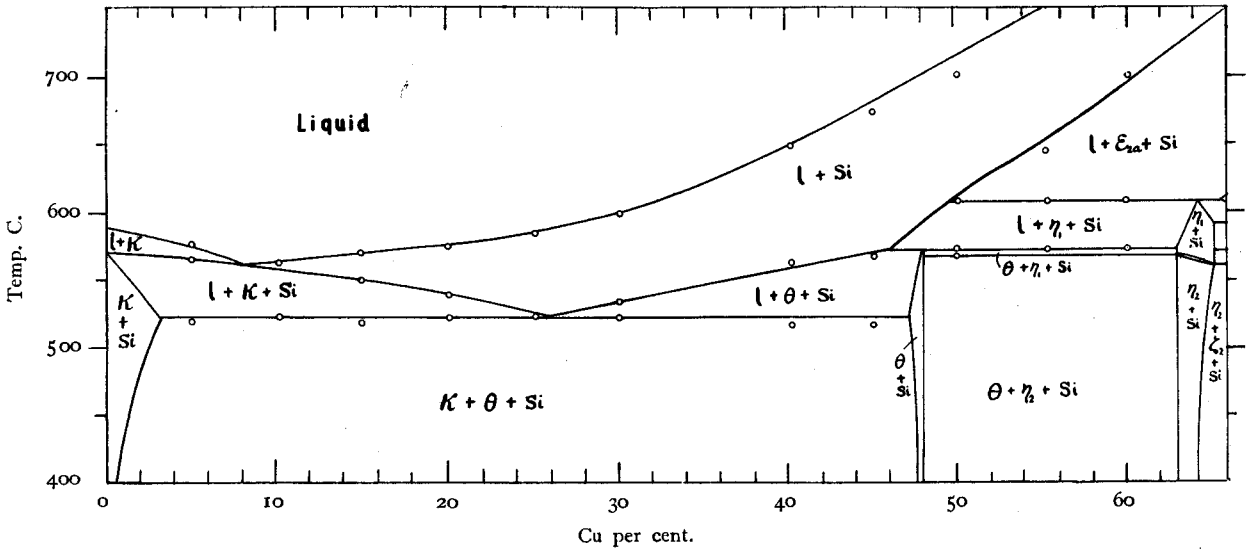

Fig. 38.

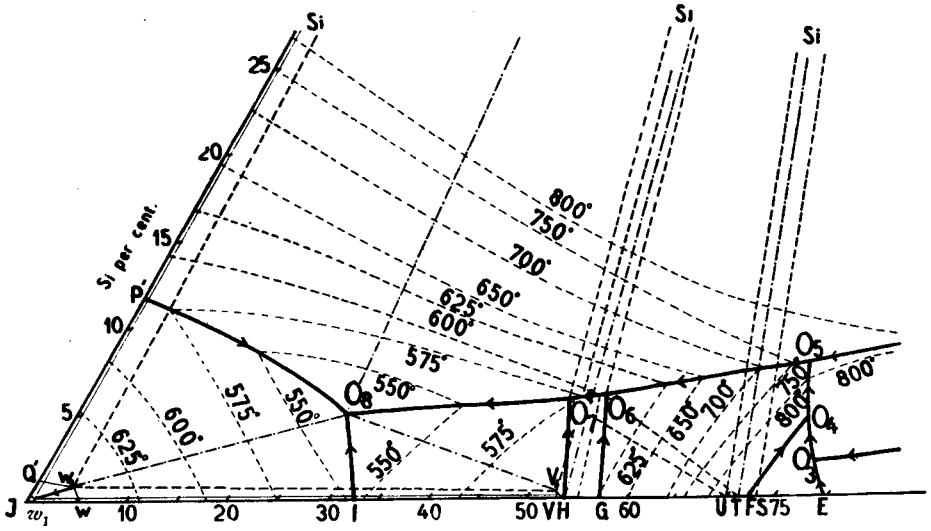

Cu per cent.

amination, but the invariant reactions which are found at 608° and 573°C. are probably peritecto-eutectic reactions;

$$\text{Liquid} + \varepsilon_{2a} \rightleftarrows \eta_1 + \text{Si}$$
$$\text{Liquid} + \eta_1 \rightleftarrows \theta + \text{Si}.$$

Another invariant reaction is observed to be a ternary eutectic at 522°C as already found by many investigators.

The composition and reacting phases of the three invariant points, O_6, O_7, O_8, on the liquid surface, are given in Table 37.

Table 37.

Point.	Composition.			Temp. °C	Reaction.	The range of reaction.
	Cu%	Al%	Si%			
O_6	52.0	42.0	6.0	608	Liquid $+\varepsilon_{2a} \rightleftarrows \eta_1 + Si$	Si STO_6Si
O_7	49.0	46.0	5.0	573	Liquid $+\eta_1 \rightleftarrows \theta + Si$	Si UHO_7Si
O_8	27.0	68.0	5.0	522	Liquid $\rightleftarrows \theta + \varkappa + Si$	Si V_1W_1Si

B. Micrographic Analysis.

In the microscopic examination of these alloys, silicon is readily identified by its colour in an unetched section, and may be distinguished from the other constituents by its crystal habit and its behaviour towards etching reagents. θ crystallizes in massive prisms and can be identified in an unetched section by its pinkish colour. It is readily attacked and becomes brownish by hot nitric acid solution.

The primary η_1 usually crystallizes in characteristic rod shape, by which this constituent can be distinguished from θ in slowly cooled specimens. Hot nitric acid attacks η_1 very little.

The primary ε_{2a} occurs in dendritic masses and appears as a highly decomposed structure, through many solid transformations. Alloys in area $JP'O_8I$ consist of aluminium, aluminium-silicon or aluminium-θ eutectic and the ternary eutectic, the relative amounts of which vary, of course, with the composition. Alloys in area IO_8O_7H consist of θ, θ-aluminium or θ-silicon eutectic and ternary eutectic. Photograph 40 shows the structure of the alloy CA 7 (44.80% Cu, 2.16% Si), in which primary θ appears as angular crystal; with silicon in the θ-Si eutectic and with aluminium and silicon in a fine ternary eutectic.

In the alloy whose composition is represented in $SiP'O_8O_7$ Si, silicon separates primarily and then eutectic reaction, Liquid$\rightarrow\varkappa$+Si or Liquid $\rightarrow\theta$+Si occurs. Finally it solidifies in a ternary eutectic reaction at O_8. The typical structure of such an alloy, containing 5.88 per cent. of silicon and 35.08 per cent. of copper, is shown in photograph 41. A portion of a crystal of primary silicon can be clearly seen in the angular form. Small lengthy silicon and black θ occur as constituents of the binary eutectic, and the fine ternary eutectic mixtures are also observed. η_1 is primarily crystallized in the alloys of GO_6O_7H; but the secondary separation differs in occuring on O_6O_7 or HO_7 according to the composition of the alloy. That is, the primarily separated η_1 is definitely determined by the micrograph, from the characteristic appearance of the rod-shaped crystals. Thus the region of its primary separation was determined. A typical structure of such an alloy TSA 445 is shown in photograph 42. In this figure we see that the primary crystal η_1 is present in the matrix of θ crystals, and silicon is observed as a constituent of the ternary complex. It has already been mentioned that the primary crystals ε_{2a} decompose into ζ and η phases. Such a structure is observed

in alloys of $FO_4O_5O_6G$ as shown previously in photograph 19.

C. The Aluminium Solid Solution.

The solid solubility of copper and silicon in aluminium has been already determined by the present writer. As it was reported in 1929*, we, therefore, found it unnecessary to describe it again.

IV. The Ternary Equilibrium Diagram of the Whole System.

Summing up the results of our present investigation, a general equilibrium diagram of the whole system is given in Figure 39, in which the reactions in solid states are omitted to avoid complexity.

Fig. 39.

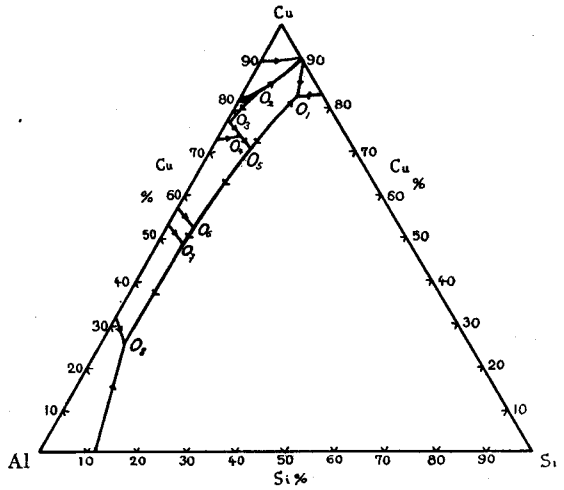

V. Summary.

(1) The author has determined the equilibrium diagram of the ternary alloys of copper, aluminium and silicon in the whole system.

(2) No ternary intermetallic compound is observed and 15 definite constituents which have been determined in each binary system were also found to occur in this ternary system.

(3) There exist 11 surfaces of the primary separations of α, β, γ_a, γ_t, ε_s, ε_{1a}, ε_{2a}, η_1, θ, χ and silicon.

(4) There are in this system 8 invariant points, O_1, O_2, O_3, O_4, O_5, O_6, O_7 and O_8, on the liquidus surface; among them 2 points are ternary eutectic, 1 point ternary peritectic, and 5 points peritecto-eutectic. The invariant reactions indicated by these points are summarized as follows.

O_1 at 727°C, Liquid $\rightleftarrows \gamma_t + \varepsilon_s + Si$,
O_2 at 980°C, Liquid $+ \gamma_a + \beta \rightleftarrows \gamma_t$,
O_3 at 910°C, Liquid $+ \gamma_a \rightleftarrows \varepsilon_{1a} + \gamma_t$,
O_4 at 840°C, Liquid $+ \varepsilon_{1a} \rightleftarrows \gamma_t + \varepsilon_{2a}$,
O_5 at 760°C, Liquid $+ \gamma_t \rightleftarrows \varepsilon_{2a} + Si$,
O_6 at 608°C, Liquid $+ \varepsilon_{2a} \rightleftarrows \eta_1 + Si$.
O_7 at 573°C, Liquid $+ \eta_1 \rightleftarrows \theta + Si$,
O_8 at 522°C, Liquid $\rightleftarrows \theta + \chi + Si$.

(5) The univariant reaction line, liquid $\rightleftarrows \gamma_t + Si$, has a maximum at about 780°C. and from this point it proceeds to both the invariant reactions, Liquid $\rightleftarrows \gamma_t + \varepsilon_s + Si$ and Liquid $+ \gamma_t \rightleftarrows \varepsilon_{2a} + Si$.

(6) Both the β phases of the Cu-Si and Cu-Al system are completely soluble in all proportions in the ternary system, and it decomposes into $\alpha + \gamma_t$; this univariant reaction line has a minimum point.

(7) Two invariant reactions, $\gamma_t + \gamma_s \rightleftarrows X + \alpha$, $\gamma_t + X \rightleftarrows \alpha + \varepsilon_s''$, are found to exist at 675° and 495°C.

(8) Five invariant reactions in solid state : $\gamma_t + \varepsilon_{2a} \rightleftarrows \delta + Si$, $\varepsilon_{2a} \rightleftarrows \delta + \zeta_1 + Si$, $\zeta_1 \rightleftarrows \delta + \zeta_2 + Si$, $\varepsilon_{2a} + \eta_1 \rightleftarrows \zeta_1 + Si$, $\zeta_1 + \eta_1 \rightleftarrows \zeta_2 + Si$ and two ternary polymorphic changes due to the $\eta_1 \rightleftarrows \eta_2$ phases, take place almost at the same temperatures as in the binary Cu-Al system.

(9) Four ternary polymorphic changes due to the $\varepsilon_s \rightleftarrows \varepsilon_s'$ and $\varepsilon_s' \rightleftarrows \varepsilon_s''$ take place at 600°, 550°, 585° and 525°C respectively.

(10) The limit of solubility of silicon and aluminium in solid copper has been determined by micrographic analysis.

Acknowledgement.

In conclusion the present writer wishes to express his sincere gratitude to Prof. D. Saito and Prof. H. Nishimura, under whose direction the present investigation was carried out.

* Suiyokwai-shi, **6** (1929)

(Received January 17, 1935).